iScience

CellPress
OPEN ACCESS

Article

Functional anatomy of the worker honeybee stinger (*Apis mellifera*)

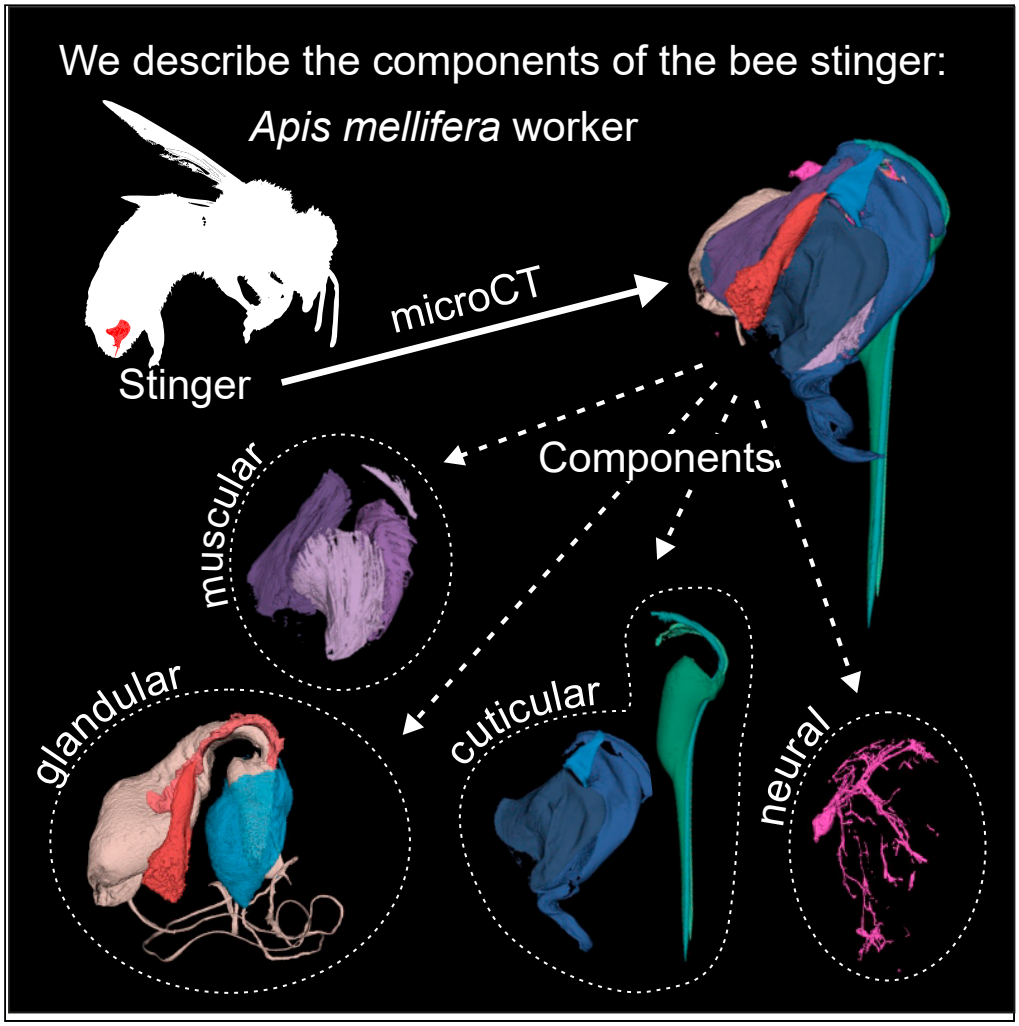

Fiorella Ramirez-Esquivel, Sridhar Ravi

f.esquivel@unsw.edu.au

Highlights

The honeybee stinger is a complex organ

Micro-CT and SEM imaging permitted detailed description and measurements

3D reconstructions clarify complex stinger geometries and spatial relationships

Neural connectivity is described with particular emphasis on *in situ* appearance

Ramirez-Esquivel & Ravi, iScience *26*, 107103
July 21, 2023
https://doi.org/10.1016/j.isci.2023.107103

iScience

CellPress
OPEN ACCESS

Article

Functional anatomy of the worker honeybee stinger (*Apis mellifera*)

Fiorella Ramirez-Esquivel[1,2,3,*] and Sridhar Ravi[1]

SUMMARY

The honeybee stinger is a powerful defense mechanism that combines painful venom, a subcutaneous delivery system, and the ability to autotomize. It is a complex organ and to function autonomously it must carry with it all the anatomical components required to operate. In this study, we combined high-speed filming, SEM imagery, and micro-CT for volumetric rendering of the stinger with a synthesis of existing literature. We present a comprehensive description of all components, including cuticular elements, musculature, nervous and glandular tissue using updated imagery. We draw from the Hymenoptera literature to make interspecific comparisons where relevant. The use of 3D reconstruction allows us to separate stinger components and present the first 3D renders of the bee stinger including the terminal abdominal ganglion and its projections. It also clarifies the *in-situ* geometry of the valves within the bulb and the spatial relationships among the accessory plates and accompanying musculature.

INTRODUCTION

Worker honeybees do not directly reproduce and their life is dedicated to the reproductive success and defense of the hive.[1] By virtue of communal-living bees make themselves an attractive target to predators by accumulating food reserves and individuals in a central location.[2] Attacks to a hive can have devastating effects, a large predator such as a bear can not only feed on honey stores and brood but also destroy the entire hive in an effort to access this valuable food cache.[3] Thus, workers need effective defense strategies against a variety of attackers and have evolutionary incentives to protect their colonies even at the cost of their own lives.[4] That is not to say that defenders automatically give up their lives but will base the decision to do so on the severity of the risk.[5]

Repelling a predator multiple orders of magnitude larger is a challenge. Bees use a variety of behaviors to repel smaller invertebrate attackers such as ants, wasps, and beetles; these include physically threatening, biting, balling, "shimmering" (producing a piping sound), body shaking (which prevents wasps from landing), or deployment of substances such as resins and propolis to bar access or imprison invaders.[6] None of these approaches are likely to be effective against larger vertebrates. Stinging represents a paradigm shift in defensive strategies compared to other physical defenses, it combines a painful venom with a delivery system that breaches the vertebrate integument to deliver it directly to susceptible tissues. Schmidt[2] likens this combination to *"an 'insect gun,' a weapon that is effective largely independent of the body size of the predator."* However, size is still a factor if stinging cannot occur in the first place, a large predator may still easily brush off a bee and crush it interrupting it mid-sting. Bees overcome this challenge through stinger autotomy, which is, detaching the stinger from the bee's body which continues to sting independently.[4] Although this is a costly strategy it is effective since whether or not the worker herself is killed or removed, the stinger will autonomously continue to penetrate into the target's tissue, injecting venom over a period of time and becoming firmly lodged and difficult to remove.[4,7] These defensive adaptations, coupled with the ability to recruit other workers through the use of pheromones, allows workers to defend against large predators by eliciting a pain response that is disproportionate to the size of a bee. The most extreme example of this is found in reports of African honeybees repelling elephants, an animal millions of times heavier, and giving chase for several kilometres.[2,8]

To be an effective defense mechanism the stinger must fulfill a number of requirements. It must pierce the highly elastic skin of vertebrates without buckling, it must pump venom quickly and efficiently, and it must coordinate the muscular contractions that generate the stinging response. To do this autonomously the

[1]School of Engineering and Information Technology, University of New South Wales, Canberra, ACT 2612, Australia

[2]Research School of Biology, Australian National University, Canberra, ACT 2600, Australia

[3]Lead contact

*Correspondence: f.esquivel@unsw.edu.au

https://doi.org/10.1016/j.isci.2023.107103

stinger apparatus must incorporate all the necessary components for stinging in a self-contained unit. This includes the muscles and cuticular structures for pumping and piercing, glandular tissue to produce and store venom and pheromones, and the sensory systems and neural circuitry that coordinates stinging. Bee stingers are, therefore, complex structures with numerous moving components. The first step in understanding how the stinger works is to understand its anatomy.

The most comprehensive description of honeybee (*A. mellifera*) anatomy, including that of the stinger, was originally published in Snodgrass'[9] landmark monograph which included detailed illustrations. Since then, imaging tools available to biologists have greatly expanded. In particular, SEM and micro-CT have become invaluable tools in describing anatomical structures in insects.[10–13] Although Snodgrass' descriptions have stood the test of time (and are indeed still being reprinted) state-of-art techniques enable significantly more detailed visualization, accurate measurements, and illustration of complex geometries in 3D space. In the intervening years there have also been many contributions that have made use of modern techniques to shed light on specific aspects of the stinger such as its material properties,[13] the ultrastructure and activation patterns of the sensory apparatus,[11] and the insertion-retraction mechanics of the stinger.[12,14] However, no modern account brings these new insights together.

Here, we build on Snodgrass' work by using a combination of high-speed imaging, light microscopy, SEM, and 3D reconstructions (micro-CT). We provide, for the first time, comprehensive 3D and SEM imagery of the worker stinger, measurements (both linear and volumetric) of the various components, and some ultrastructural features. We review the functional implications of our anatomical observations drawing from modern studies on the honeybee stinger and ovipositor use in other Hymenoptera including other *Apis* species. This detailed description aims to provide comprehensive modern imagery and capture the current state of knowledge as a basis for future studies on the bee stinger.

RESULTS AND DISCUSSION

Stinger function and components

The stinger of the worker bee is small, reaching approximately 2.5mm in length (Figures 1A–1C). It is derived from the modification of the ovipositor.[15] Over evolutionary time the bee stinger has become a purely defensive organ and is no longer involved in egg laying.[15–17] Its primary function is to deliver venom into an aggressor to either kill or deter attacks on the hive.[4] Stinging of vertebrate attackers can lead to autotomy, which can result in the death of the worker.[18–20]

When stinger autotomy occurs, the stinger is left embedded in the tissue of the attacker and continues to sting for a short period of time.[4] In order to achieve this autonomous function, the autotomized stinger contains all the necessary components for stinging (illustrated in Figure 1D): the piercing and pumping parts, accessory plates to support musculature, the terminal ganglion (which regulates piercing behavior), as well as the venom glands, venom sac and glands responsible for producing alarm pheromone (Koschevnikov's gland). The latter is important as once an intruder has been stung by a worker, the stinger also secretes alarm pheromones to recruit additional workers to defend the hive and attack the intruder.[7,21]

Insertable length

Piercing

During stinging, only the distal end of the stinger is inserted into tissue. This portion of the stinger is comprised two lancets and a stylet, as described by Snodgrass,[22] in SEM the whole assemblage can be observed in great detail (see Figures 2A and 2B). While the lancets have a harpoon-like profile the stylet has a beveled tip and is ventrally deflected on its distal end (Figures 2C and 2D). The gross morphology of these components is very similar to that of *Apis cerana*, which has been previously illustrated in SEM.[12]

To penetrate tissue, the lancets protract and retract past the tip of the stylet in an alternating fashion, gradually propagating deeper over several strokes (see Video S1). During lancet retraction, stinger penetration is believed to be aided by the rearward facing lancet barbs which dig into tissue on retraction thus anchoring that lancet and allowing the other components to penetrate further.[23,24] As the stinger penetrates, venom issues from between the lancets (Figure 2E, see "venom canal"). Digitization of the high-speed videos indicates the lancets move at antiphase to each other (see sample data in Figure 6F).

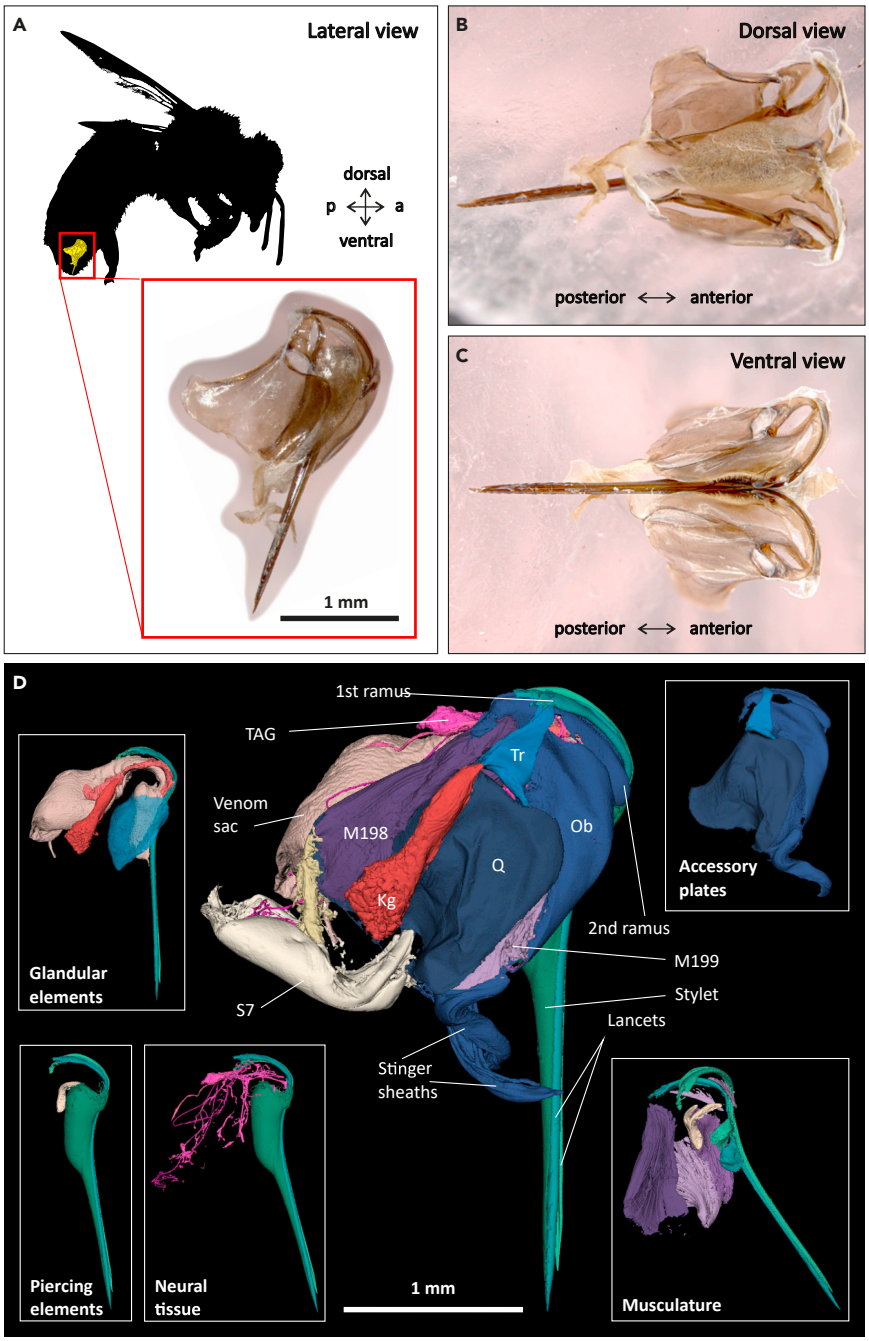

Figure 1. Components of the stinger of the *Apis mellifera* worker

(A) The location, size, and orientation of the stinger apparatus within a worker bee is illustrated in lateral view. Light microscopy images of the stinger with venom sac excised and soft tissues removed through NaOH digestion.

(B) dorsal view.

(C) ventral view.

(D) 3D reconstruction of the stinger based on micro-CT data, the larger image displays some of the salient structures including: Koschevnikov's gland (Kg), the lancet protractor and retractor muscles (M198, M199), oblong plate (Ob), quadrate plate (Q), the 7th sternite (S7), the terminal abdominal ganglion (TAG), triangular plate (Tr).

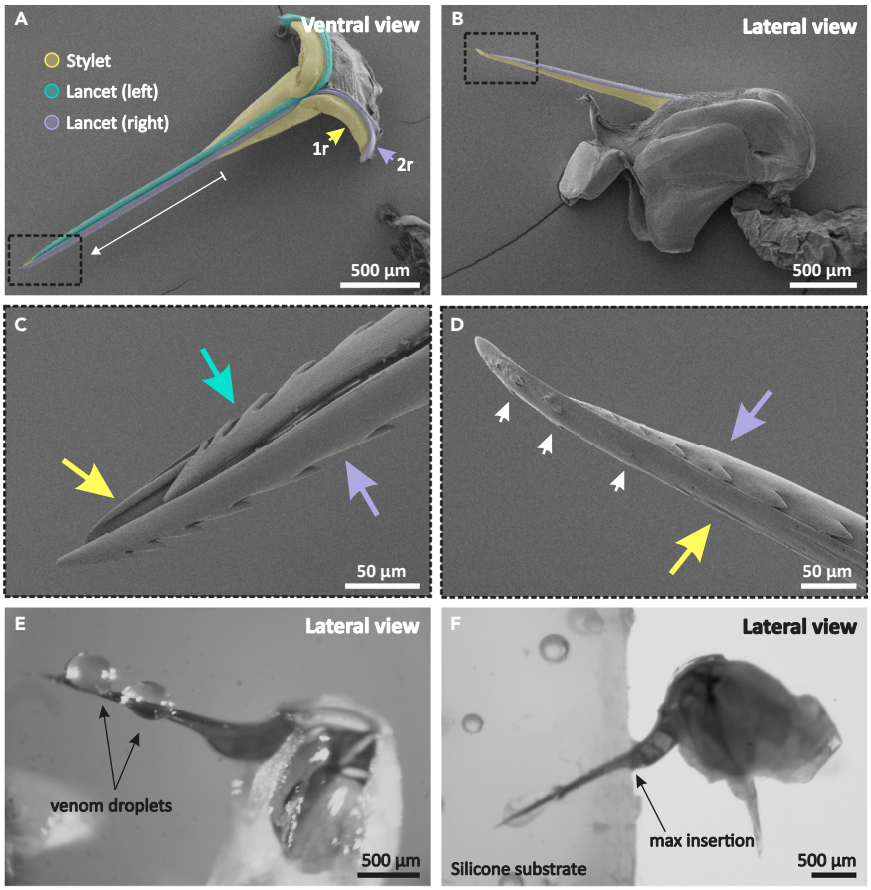

Figure 2. Piercing parts of the honeybee stinger

(A) The insertable length (white arrow) is comprised two lancets and a stylet, the former are continuous with the first rami (1r) and the latter articulates with the second ramus of the oblong plate (2r) on either side; note that the accessory plates have been removed.

(B) On a lateral view it is possible to observe the stinger in is retracted configuration nestled among the accessory plates.

(C) Rearward facing barbs of the lancets (magnified area from panel A).

(D) Blunt, deflected tip of the stylet with small stylet barbs, white arrows (magnified area from B).

(E) Venom seeps between the lancets, distally from the bulb but not from the tip of the stinger.

(F) Penetration into tissue or, in this case, artificial substrate is limited by the widening of the stinger bulb (single frame from high-speed videography of stinging behavior).

Although further detailed analysis of the kinematics is necessary, preliminary observations are consistent with the broad patterns of stinging qualitatively described earlier in *A. mellifera*.[25]

The extent to which the stinger penetrates into tissue appears to be limited by the expansion of the stylet into the bulb. Over the course of 24 stinging trials recorded here the bulb was never inserted into the substrate (example frame shown in Figure 2F). This observation is also consistent with the stinging behavior of *A. cerana* described in a previous study.[12] Consequently, for the purposes of this study, we define the insertable length as the portion of the stylet distal to the bulb (see Figure 3A). This can be measured in dorsal view from the distal tip of the stinger to the first widening of the bulb. Where the bulb first arises, there is a "wrinkle" in the cuticle and this was used as a landmark to measure the end of the insertable length. Our measurements showed the honeybee insertable length to be 1320 $\pm$ 61 µm (mean $\pm$ s.d., n = 10, measured in SEM specimens). The stinger insertion of *A. cerana* has been described as being perpendicular to the substrate or nearly so,[12] if this is also the case in *A. mellifera* this means that the maximum distance that the stinger may penetrate into tissue is approximately 1.3mm. In human skin this would be sufficient to penetrate the epidermis and inject venom into the underlying dermal layer but not into the subcutaneous tissue.[26,27]

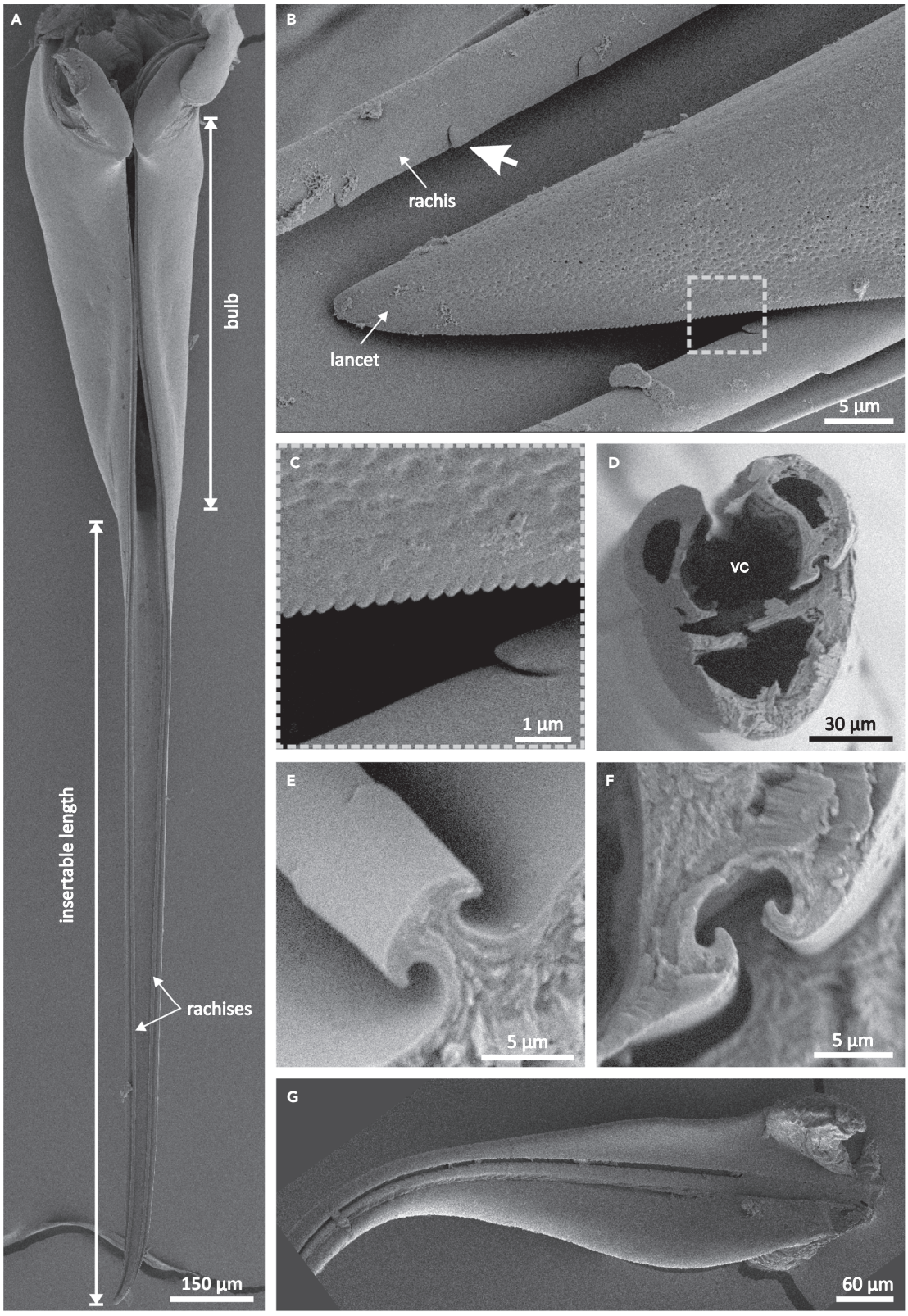
A
bulb
insertable length
rachises
150 µm
B
rachis
lancet
5 µm
C
1 µm
D
vc
30 µm
E
5 µm
F
5 µm
G
60 µm

Figure 3. The olistheter of the stinger, comprised the rachises of the stylet and the aulax of the lancets

(A) The stylet showing the insertable length and bulb with lancets and rami removed, the rails (rachises) of the olistheter can be seen along its length.

(B) The rachises bear minute rearward facing notches (white arrow head), the scalloped edge of the lancet can also be observed (insert).

(C) Magnified area from previous panel shows the scalloped edge of the lancet.

(D) The olistheter assembly can be observed in a cross-section of the stinger tip. The stylet and lancets form a hollow canal through which venom flows, the venom canal (vc), the hollow insides of the lancets and stylet do not carry venom (image courtesy of Claudia Klose).

(E) Rachis of the stylet.

(F) Aulax of the lancet.

(G) Aulax continuation on the interior margin of the first ramus.

The reciprocating lancet action is conserved across a variety of hymenopterous insects piercing widely different substrates including wood, fruit, insect tissue, and mammalian skin.[23–25,28] The range of prey, host species and oviposition sites that Hymenoptera utilize translates into a large range of functional specializations and ovipositor morphologies. Quicke et al.[29] carried out a comprehensive comparative study of the lancet and stylet cross-sectional anatomy revealing a wide range of morphologies. Analyses of the insertion mechanics postulate that the reciprocal action puts one lancet in tension while the other is in compression, stabilizing the piercing parts and preventing buckling.[23,24] This insertion strategy seems to be so versatile that in some species long ovipositors have evolved to become highly steerable within substrates via the differential extension of the two lancets.[23]

The piercing parts of the honeybee stinger need to pierce into elastic tissue without buckling or breaking. Aside from the reciprocating action of the lancets the material properties of the stinging parts also assist in fine-tuning performance. The aculeus of *A. mellifera* has been shown to have variable elasticity and hardness along its length.[13] The maximum elastic modulus is found at the proximal end of the insertable length, which experiences the largest bending stresses, while the distal end exhibits the minimum elastic modulus.[13] This variability in material properties is thought to be achieved via metal enrichment of the cuticle with iron, copper, and manganese.[30]

Barb geometry

The lancets and stylet all possess barbs although those of the lancets are much more pronounced (see Figure 2D).

The lancets bear, on average 10 barbs each (n = 10 workers, measured on the left lancet). In one case, we noted a lancet with 9 barbs. The first barb arises, on average, 53μm from the tip; distally the barbs are closely spaced together but they become more spaced out toward the bulb (see Table 1). Previous studies have reported tighter spacings between the barbs.[31,32] However, trait variability may be due to differences in imaging resolution (previous studies used light microscopy, while the present study measured barbs from SEM images), variability on measuring protocols or genetic differences between populations. The length of the lancet barbs varies with the first and last two barbs being shorter than the rest (see Table 2).

The stylet barbs are found on the dorsal aspect (Figure 2D). These barbs are much less pronounced and quite variable in size (see Table 3) and numbers, there may be one to four pairs on the distal end of the lancet. The stylet barbs of *A. cerana* appear to be much more pronounced than those of *A. mellifera*.[14]

The barbs in both lancets and stylet are rearward facing with respect to the penetration direction. This has been shown to decrease the force required for penetration and increase the force required for extraction.[12,14] Measurements from Ling et al.[14] indicate that the extraction force of the *A. cerana* stinger is approximately 20x larger than the insertion force. Similarly large ratios between extraction and insertion forces would be expected in *A. mellifera* given the morphological similarities of their stingers[31,32] and their even greater propensity to autotomy compared to *A. cerana*.[19] Although other species also display similar barbs they tend to be less markedly hooked and can be sheathed within the margins of the stylet when retracted, which is not possible in *A. mellifera* workers (Figure 2C).[12,33] The number and profile of the barbs is thought to influence rates of autotomy in different Hymenoptera.[34]

The olistheter

The stylet supports the two lancets which move independently in a reciprocating manner to pierce and penetrate into tissue.[25,35] This movement is achieved in part by means of the olistheter, a set of rails that couples the lancets to the stylet via a tongue and groove mechanism that has been described in a

Table 1. Lancet barb distribution, n = 10 workers

Distance between barbs (um)	Average	std dev
Tip to 1	52.6	6.4
1 to 2	23.6	3.0
2 to 3	29.5	2.0
3 to 4	38.4	5.1
4 to 5	47.1	3.4
5 to 6	60.3	4.8
6 to 7	70.3	6.4
7 to 8	84.0	6.2
8 to 9	105.5	11.7
9 to 10	143.6	19.0

range of Hymenoptera.[15,29,36–38] The olistheter allows the lancets to slide over the stylet in a reciprocating motion while limiting motion to a single axis[29] (Figure 3).

In the case of the honeybee, the tongue or rachis projects from the surface of the stylet and runs along its entire length (Figures 3A and 3B). Our imaging showed that the rachis bears small lateral notches standing approximately 0.3–0.5μm above the surface throughout its length, these are spaced about 15 to 20μm from each other and are offset on either side of the rachis (Figures 3B and 3C). The orientation of these notches is such that it appears to facilitate the lancet extension and provide resistance to retraction. Because of their small size they are only observable using SEM and have not previously been described in *A. mellifera*. However, Matushkina and Stetsun[37] described similar structures in the digger wasp *Oxybelus uniglumis* (Hymenoptera, Crabronidae) although these structures appear more pronounced in this species.

The complementary groove on the lancet which accepts the rachis is called the aulax. Viewed in cross-section the aulax displays a recurved lip, which closely matches the profile of the rachis, providing a secure engagement between the two parts (see Figures 3D–3F). The aulax extends throughout the length of the lancet. Even as the lancet broadens to form the second ramus (Figure 2A), which articulates with the accessory plates, the aulax can still be observed on the interior margin of the ramus (see Figure 3G).

Venom canal

Apart from piercing and penetrating into tissue the insertable length delivers venom into the tissue of the target. The stylet and the two lancets come together to form the venom canal as a tripartite tube (Figure 3D). The lancets make up the majority of the perimeter with the stylet creating a seal on the dorsal side (see Figure 2C). The ventral margin does not seal completely, this allows venom to seep through the seam between the lancets, below the level of the bulb, toward the distal end of the insertable length (see Figure 2E and Video S1). Unlike a hypodermic needle venom does not issue from the distal tip of the aculeus. In cross-section, the lancets and stylet are also hollow structures but this is a consequence of development and these channels do not carry venom.[22] In the absence of a substrate, we observed beads of venom forming along the insertable length (Figure 2E) but never issuing from the apex of the stinger or from the region of the bulb.

The venom canal has an average internal diameter of 39 $\pm$ 4.5μm (n = 14 workers) and it does not appear to change diameter along its length (see Figure 4). The canal diameter was measured using physical cross

Table 2. Lancet barb lengths (μm)

	Barb 1	Barb 2	Barb 3	Barb 4	Barb 5	Barb 6	Barb 7	Barb 8	Barb 9	Barb 10
Average	12.0	18.2	21.7	22.1	21.6	22.4	21.3	20.4	17.2	11.5
Std dev	2.2	2.0	2.6	3.0	3.0	2.4	3.8	3.8	5.7	3.0
n	10	10	10	10	10	10	10	10	10	7

Barb length was measured in 10 worker specimens, except for barb 10 where one specimen only had 9 barbs and 2 further specimens were not suitable for measurement at the last barb.

Table 3. Stylet barb lengths (μm)

	Barb 1	Barb 2	Barb 3	Barb 4
Average	8.3	10.4	10.3	3.6
Std dev	2.2	4.0	3.4	
n	5	4	3	1

section in SEM specimens or optical cross-sections in micro-CT specimens. Although some variability in diameter was observed there was no consistent trend for the venom canal to either increase or decrease along the insertable length.

Ultrastructure

The lancets and stylet both have a finely pitted surface that can only be observed at high magnification (Figure 3C). There are also extremely fine serrations that can be observed on the margins of the lancets. These have been previously observed by Weyda and Kodrík,[39] the dimensions reported in their study are in close agreement with our observations (Table 4). Weyda and Kodrík[39] hypothesize that the pitted surface and serrations serve to maximize tissue damage on insertion and therefore aid in venom penetration. However, at present there is no experimental data to confirm this hypothesis.

Stinger autotomy

Natural worker stinging behaviors were not observed during this study. However, previous authors report that stinger autotomy usually results in the death of the worker but this may not occur for up to 18 to 114 h during that time it may continue to defend the hive.[7] As the stinger is torn away from the body the lower digestive tract may also remain attached to the stinger but how much, if any, is quite variable and this may influence how long a worker survives after autotomy.[19] The stinger is attached to the interior of the body cavity by three sets of muscles, which are atrophied compared to other aculeate Hymenoptera, further facilitating autotomy.[19,40] In order for a honeybee to extract its stinger without autotomy it must rotate its body clockwise or anticlockwise around the sting site to pry the stinger loose, this behavior may successfully remove the stinger without autotomy but can be quite laborious.[19]

Although common in *A. mellifera* stinger autotomy is not completely unique to this species,[4] it is also known to occur in other bees in the genus *Apis*,[19] ants in the genus *Pogonomyrmex* and potentially a few other genera,[18] and some wasps in the tribes Epiponini, Polistini, and Rhopalidiini.[33,34,41,42] Some *Vespula* wasps have also been shown to lose their stingers in vertebrate tissue if the wasp is forcibly removed but the wasp cannot undergo autotomy unaided.[43] Notably, solitary bees do not exhibit stinger autotomy.[30]

Bulb and valves

The bulb is a dorsal widening of the stylet (Figure 3A) which houses the venom pumping structures, the valves (Figures 5A–5C), and receives venom from the venom sac when stinging is initiated.[22,40] Although Snodgrass[22] described the bulb and valves, so far there has not been clear imagery of the interior of the bulb and the configuration of the valves within it.

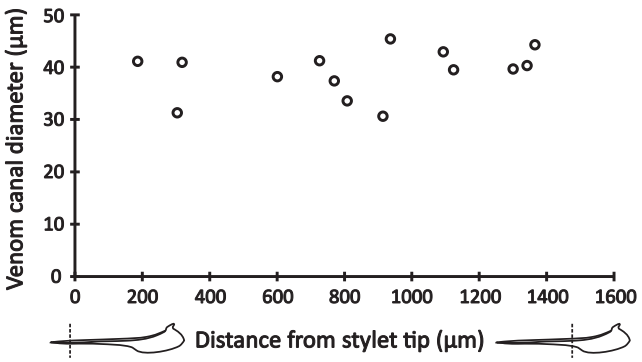

Figure 4. Internal diameter of the venom canal
Measured in micro-CT and SEM images.

Table 4. Lancet tooth and surface pitting dimension, all given in μm (mean ± std dev)

Source	Tooth height	Inter-tooth distance	Pit width
Weyda and Kodrík[39]	0.16 ± 0.02 (n = 5)	0.26 ± 0.03 (n = 5)	0.06 to 0.4
Present study	0.115 ± 0.025 (n = 11)	0.328 ± 0.038 (n = 15)	0.059 to 0.370

SEM and micro-CT imaging performed here reveal that the bulb is lined by a smooth membrane, which is continuous with the membrane of the venom sac (Figures 5A–5D). Distally this lining narrows within the bulb more abruptly than the cuticle to funnel venom out of the bulb (Figures 5B and 5D). The region within the bulb lining accommodates a small volume of venom (see Table 5). The cuticle of the bulb is relatively thick and multilayered compared to the lining membrane (Figure 5F).

This bulb lining can be observed in other Hymenoptera.[38,44] Packer[44] mentions that in the Apoidea the internal surface of the bulb is often narrower than the exterior. This is not always the case across the Hymenoptera as in some cases the bulb itself is not as pronounced.[12,35] Austin and Browning[45] surveyed the interior of the ovipositor of species across different orders and found that the majority of surveyed insects displayed posteriorly facing scales on the inner surfaces of the ovipositor. These scales aid in shifting eggs down the ovipositor acting as "linear ratchets" but these are not observed in honeybee workers.[45] The inner lining of the bulb in worker bees is completely smooth (Figure 5), which is consistent with the loss of egg-laying function of the stinger in aculeates.[15,16]

The bee stinger delivers venom rather than eggs like in other species. Across the Hymenoptera there are different strategies to deliver fluids through the ovipositor. Piek[16] identified two different modalities of venom delivery in the aculeates, the valve mediated type (employed by Sphecidae, Apoidea, and Formicidae) and the injection type, which relies on muscular contraction of the venom sac (employed by Vespidae and Pompilidae). Honeybees employ the valve mediated strategy although the details of venom flow through the stinger are not well understood. Additionally, due to the small diameter of the venom canal it is likely that capillary action plays a role in venom flow.

The valves of *A. mellifera* consist of a complex cuticular structure projecting ventrally from the dorsal aspect of each lancet (Figure 5B). Each of these structures is made up of two parts, a pouch that resembles a posteriorly facing chitinous cup, sometimes referred to as the boss,[46] and two semicircular membranous appendices that project medially[40] (see Figures 6A–6C). The elements that compose a valve and its location are extremely variable across the Hymenoptera and even within Apidae there is significant variability.[46] In light microscopy the valves appear translucent and extremely fragile (Figure 6C) while in an SEM the valves often appear collapsed, likely a result of shrinkage in the drying process (Figure 6D). Micro-CT preparations permit viewing of the valve orientation relative to each other within the bulb but suffer some dehydration artifacts as in SEM imaging. In micro-CT it is possible to observe the boss of the valve sits medially with two flexible wings projecting contralaterally to the supporting lancet (Figure 5A). Optical sections through the valve enable visualization of the internal structure of the valve, which is quite complex (Figure 6E). There are closed chambers within the proximal portion of the valve and the cuticle varies in thickness greatly. Although the chambers appear separate in the figure these merge to form a single cavity ventrally. These features may influence how the valve behaves causing it to collapse or hinge in specific ways as it moves through liquid (venom). The valves are extremely small and difficult to manipulate with the valve pouch measuring 222 ± 15μm (n = 4) in the dorsoventral axis, the interior depth of the pouch was 108 ± 7μm (n = 4), and the membrane measured 87 ± 3μm (n = 4) at its maximum length.

Our own high-speed videography appears to indicate that the valves pump in antiphase to each other and have to forcibly push past each other as their strokes intercept roughly midway down length of the bulb (Figure 5E). It is not yet entirely clear how the stinger generates net outflow using bidirectional pumping and this merits further investigations.

The venom pumping structures are referred to using a range of different terms including valves,[22] lancet valves,[11,47] valvilli,[37,46,48] or valvular lobes.[31,32,40] These are a feature unique to some families of Hymenoptera and is not observed in other insect orders.[46] Even among the Hymenoptera these structures have diverse geometries, functions (e.g. aiding in egg delivery), and may be positioned at various points along the lancet.[46] It is worth clarifying that although these structures are sometimes called "valves," based on their form and

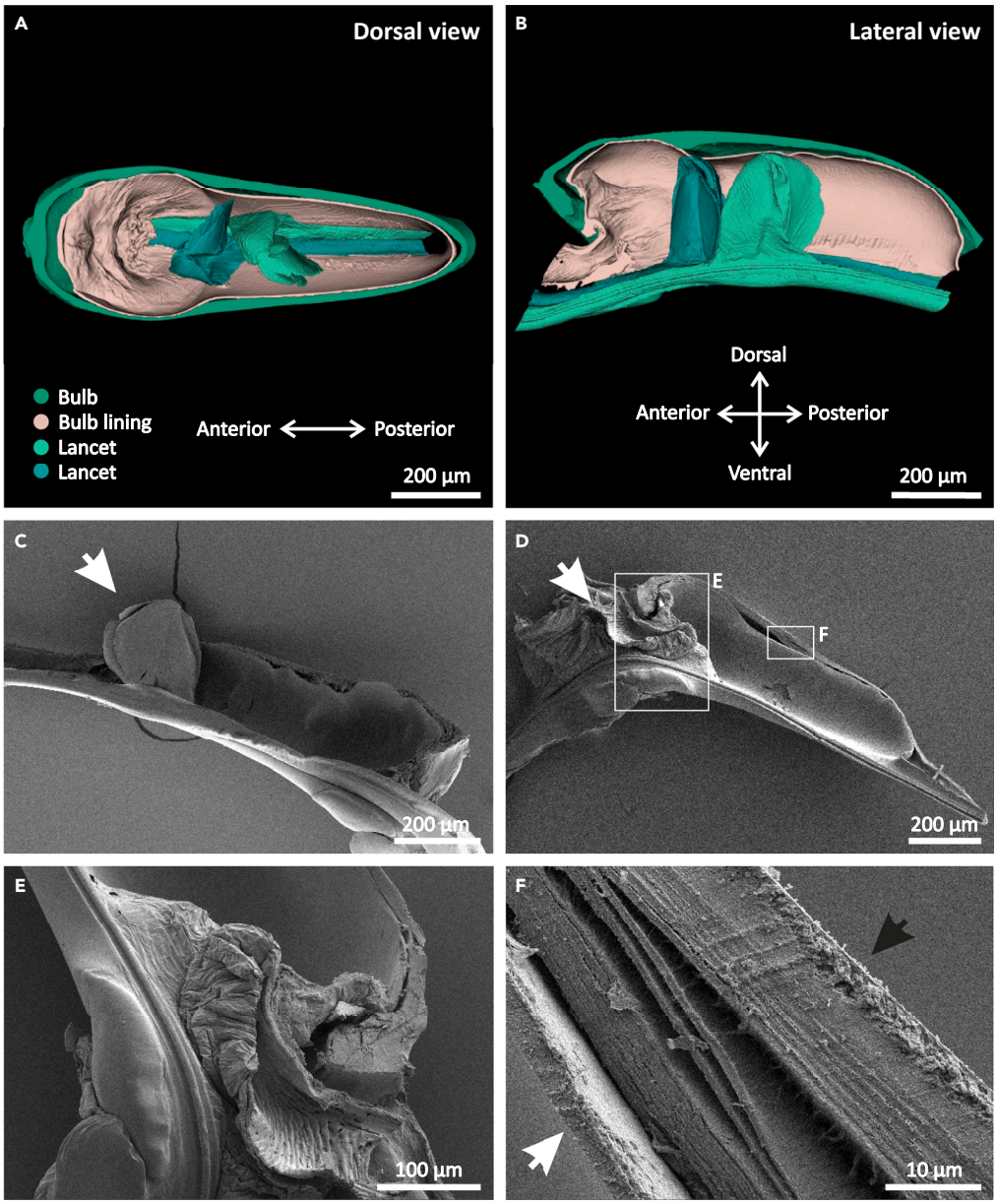

Figure 5. The bulb of the stinger, formed by the dorsal widening of the stylet, houses the venom pumping valves

Micro-CT reconstructions of the bulb and valves (A) optical frontal section showing the ventral half of the bulb.
(B) Optical sagittal section showing the right half of the bulb.
(C and D) Physical sagittal sections of worker bulb showing a consistent lining arrangement to the micro-CT reconstruction.
(C) Bulb sagittal section with one lancet and valve included (white arrow head).
(D) Bulb sagittal section without lancets showing the bulb lining is continuous with the venom canal and venom sac, white arrow head indicates remains of the venom canal/venom sac.
(E) Inset showing detail of bulb lining-venom canal tissue.
(F) The bulb wall is relatively thick, layers of outer cuticle (black arrow) and membrane lining (white arrow).

presumable function in the honeybee noted here they likely function as collapsible pistons rather than valves as they pump venom through the venom canal.[22,40,44,46] While a valve regulates or directs flow a piston actively creates positive pressure to pump fluid. The term "valve" here is a derivation from valvifer, as in the basal plates in an insect's ovipositor, but it does create some confusion when referring to its function. Having noted this nuance, we will continue to refer to this component as the valve for consistency with existing literature.

Table 5. Summary dimensions of the bulb, dimensions are given in μm unless otherwise stated

	Mean	SD	n
Bulb length	786	27	7
Bulb width	320	16	10
Bulb depth	266	25	7
Bulb volume (mm^3)	0.028		1

Measurements collected from SEM and micro-CT imagery.

The valve is attached to the proximal portion of the lancet. The lancet also supports the piercing barbs anteriorly and is continuous with the first ramus, which articulates with the accessory plates (see Figure 6F). Consequently, piercing and pumping occur simultaneously and it is not possible to decouple these two functions. Power for both of these movements is provided indirectly by contraction of muscles supported by the accessory plates. The effect of their contractions is transferred to the lancet via the triangular plate and first ramus. This mechanism has been previously described in *A. mellifera*[25] and more recently, to a greater level of detail in the parasitoid wasp *Diachasmimorpha longicaudata* (Braconidae).[35] It is interesting to consider that this obligately coupled actuation may facilitate autonomous function during autotomy by eliminating the need for two separate sets of muscles (e.g., as seen in injection type venom delivery systems), which may be more metabolically costly.

Accessory plates and musculature

The lancets, responsible for pumping and piercing of the stinger, are actuated by muscles attached to the accessory plates (Figures 7A and 7B). These cuticular plates are bilaterally symmetrical consisting of a triangular, quadrate, and oblong plate on each side. Additional cuticular elements and muscle groups are responsible for protraction of the aculeus from its resting position nestled between the accessory plates. Ogawa et al.[25] described these motions by studying muscle attachment sites and the pattern of neural activation of muscle groups. We extended on their work by carrying out direct observations of the plate motions using high-speed videography, examining micro-CT preparations with different lancet protraction-retraction states, and replicating plate motions using a 3D printed physical model (Figure S1). Additionally, we provide further detail on muscle attachment sites and 3D renders of the accessory plates. Although 2D illustrations are extremely useful, it can be very challenging to visualize a complex, dynamic, 3D structures from drawings alone. Muscles groups are described using the nomenclature of Ogawa et al.[25]

Protraction and retraction of the lancets

The triangular plate articulates through flexible cuticular articulations with three different parts of the stinger (Figure 7C). The anterior point of the triangular plate is continuous with the first ramus (Figures 7D and 7E) and forms a stiff articulation (see Video S1 and Figure S1). The lateral and medial points of the triangular plate articulate with the quadrate and oblong plates, respectively, to form hinge joints (Figures 7F and 7G). The triangular-oblong plate joint provides the central pivot point for lancet extension and retraction movements (see Video S1 and Figure S1).

Movement of the lancet is mediated by the protractor muscle M198 and the retractor muscle M199. The protractor muscle M198 originates on the anterior dorsal corner of the oblong plate and fans out to insert on the dorsal corner of the quadrate plate on both medial and lateral aspects of the plate (see Figure 8). Contraction of this muscle shifts the quadrate plate over the oblong plate toward the rami causing the triangular plate to pivot, this pushes the ramus posteriorly and protracts the lancet (see Figures 8E and 8F). The retractor muscle M199 originates on the oblong plate at the base of the stinger sheath and fans out widely to insert on the medial aspect of the quadrate plate (see Figure 8F). Contraction of this muscle returns the quadrate plate to its resting position causing the triangular plate to pivot back and retract the lancet.

The oblong plate is closely associated with the ramus, which is continuous with this structure and is connected along most of its length via a fine translucent membrane (Figure 7A). Two similar fine, translucent membranes span the gaps between the triangular and oblong plates and the triangular and quadrate plate. These can be seen clearly when comparing light microscopy and SEM images as the membranes are opaque to electrons but transparent to light (Figures 7A and 7B).

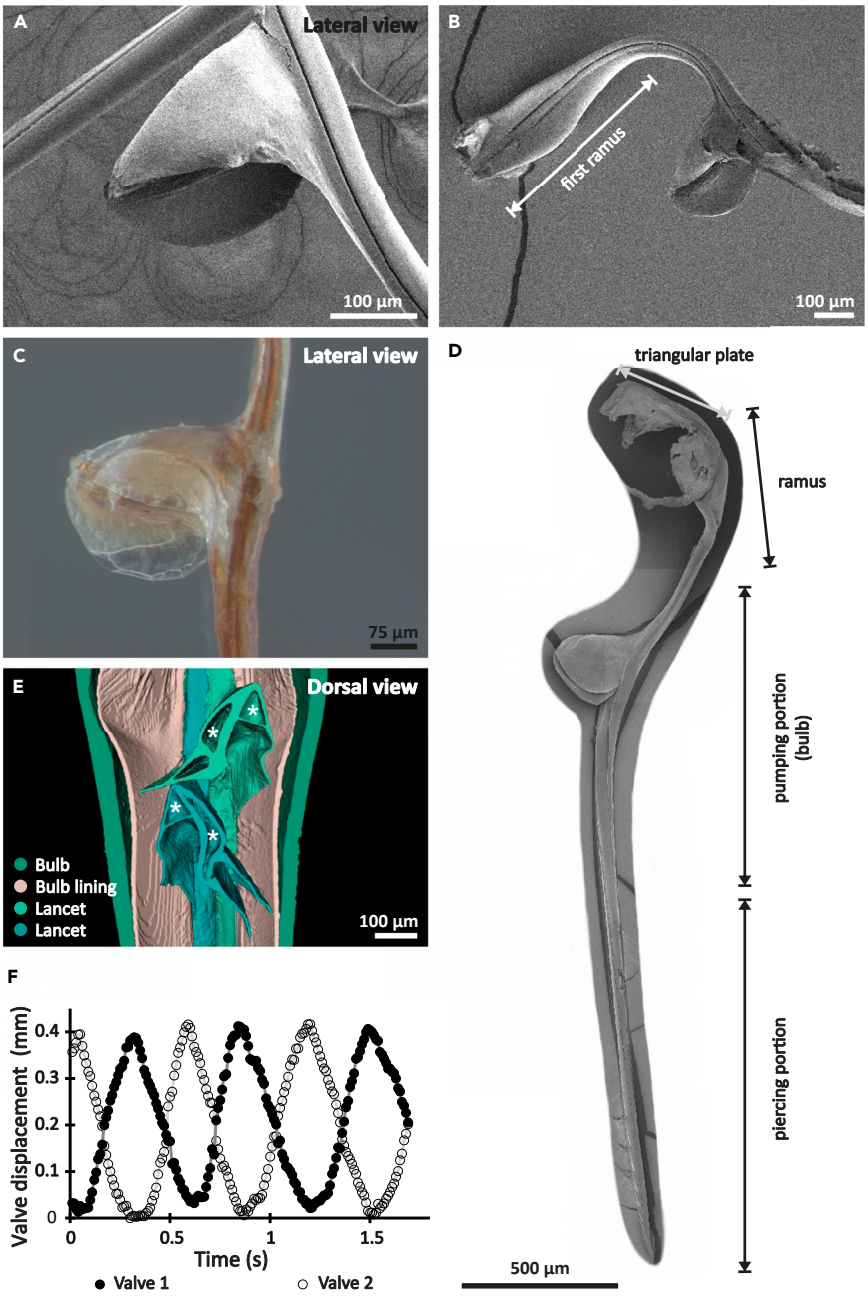

Figure 6. The lancet valves

(A) The lancet valve is comprised a rigid cup-like structure and two thin semicircular appendages.

(B) The lancet is continuous with the first ramus.

(C) In light microscopy the very thin delicate structure of the valves can be better appreciated.

(D) The different roles of the lancet can be understood when viewed separately from the stylet, the distal end of the lancet pierces into tissue, the central portion bears the valves that project into the bulb and the proximal end broadens to form the first ramus, which slides along the second ramus and articulates with the triangular plate.

(E) A frontal section of the stinger valve shows the interior of the valves and displays the variable thickness of the cuticle and enclosed chambers (*) within the boss of the valve.

(F) Preliminary analysis of the valve pumping action from high-speed videography shows the two valves pump in antiphase to each other; "valve displacement" refers to the single axis displacement along the length of the bulb.

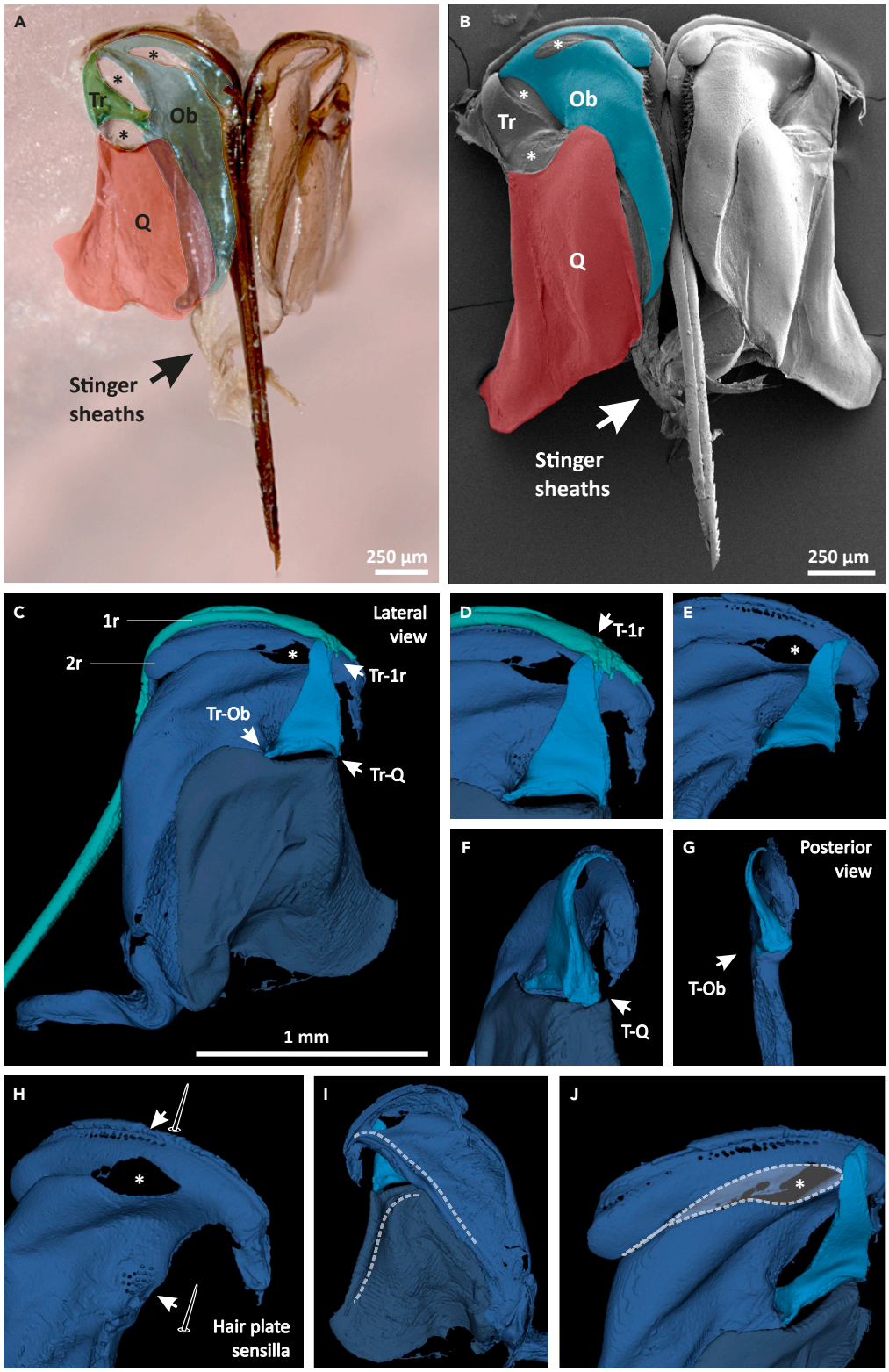

Figure 7. The accessory plates of the stinger

(A) In light microscopy the triangular (Tr), quadrate (Q), and oblong (Ob) plates appear translucent and are connected to one another by extremely fine transparent membranes (*).

Figure 7. *Continued*

(B) In SEM imaging the same connecting membranes (*) appear opaque and are difficult to identify.

(C) micro-CT reconstruction of the plates displays articulations between Ob-Tr-Q and Tr-first ramus (1r).

(D) The triangular plate-first ramus articulation is made of continuous cuticle and difficult to visualize.

(E) The triangular pate does not attach to the second ramus.

(F and G) The triangular-quadrate plate articulation and the (G) triangular-oblong plate articulation are both simple hinge joints.

(H) Holes in the second ramus and oblong plate can be seen where hair plate sensilla would be.

(I) Hashed lines highlight thickened areas of the plates; these provide additional stiffness.

(J) The hashed line outlines the position of the very thin layer of tissue that connects the posterior margin of the second ramus and the anterior margin of the oblong plate.

Protraction and retraction of the aculeus

An additional set of muscles control movement of the aculeus from its resting position between the accessory plates to its protracted, stinging position. These movements involve an additional, Y-shaped, cuticular element, the furcula, which provides a site for muscle attachment. The furcula is positioned on the dorsal surface of the bulb (Figure 8D). The furcula muscles M197 originates on the medial aspect of the oblong plate and inserts into the furcula. Its bilateral contraction protracts the bulb away from the accessory plates. The antagonistic muscles M196 originates on a tuberosity on the ventral anterior side of the bulb and inserts in a fanned fashion into the medial aspect of the oblong plate, on the 2nd ramus (Figure 8D). Its contraction retracts the bulb back between the accessory plates. Examples of stingers in the retracted and protracted positions can be seen in Figures 2B and 2G, respectively (also see Video S1).

Comparison with other hymenoptera

Our observations here have been consistent with the work of Ogawa et al.[25] Their study is unique in having described the pattern of neural activation of muscle groups. Other descriptions of the protraction and retraction of the lancets in various Hymenoptera exist in the literature,[35,47,49,50] but these are generally based on detailed anatomical analysis of the articulations and muscle groups. Detailed *in-vivo* imaging that reveals muscle activation is quite challenging in species that do not undergo autotomy although some authors work around this problem by making use of modern imaging techniques to capture snapshots at various stages of lancet extension and retraction.[35]

Van Meer et al.[35] describe the musculature and ovipositor mechanics in a much smaller species, *D. longicaudata* (body length = 5mm) using detailed micro-CT imagery. Their descriptions are largely consistent with the gross mechanics described here despite the size difference in study species, and the fact that *D. longicaudata* is a parasitoid wasp and does not sting vertebrates. The cuticular elements of *D. longicaudata* vary from those of *A. mellifera*, however, analogous structures can be easily recognized and the key muscle groups seem to function very similarly. Exceptions are the muscles that the authors call 1vlf-gm, M-1vlf-A and M-1vlf-B, which are missing from *A. mellifera*. However, these are all quite small and do not appear to play a major role in ovipositor actuation. 1vlf-gm is the largest of the three and interestingly appears to connect the proximal ends of the two lancets. In *D. longicaudata* this muscle is hypothesized to play a role in stabilizing the stinger.

Nervous system

The muscular contractions that generate stinging behaviors are orchestrated by the terminal abdominal ganglion (TAG).[11,25] Electrophysiological studies by Ogawa et al.[11,25] indicate that the complementary muscular contractions required for stinging are generated by a central pattern generator consisting of a pair of oscillators in the TAG. Their experiments strongly imply that propriosensory input from sensory sensilla is necessary for the coordinated action of the stinging muscles. In these works, removing input from propriosensory sensilla did not lead to a cessation of stinging but led to a partial loss of coordination, conversely stimulation of sensory sensilla triggered a stinging response.

Sensory sensilla

Stinger propriosensory input is provided by sensory sensilla visible on the surface of the honeybee stinger.[11,25,50] These are comprised fields of hair plate sensilla and campaniform sensilla recorded here in SEM.

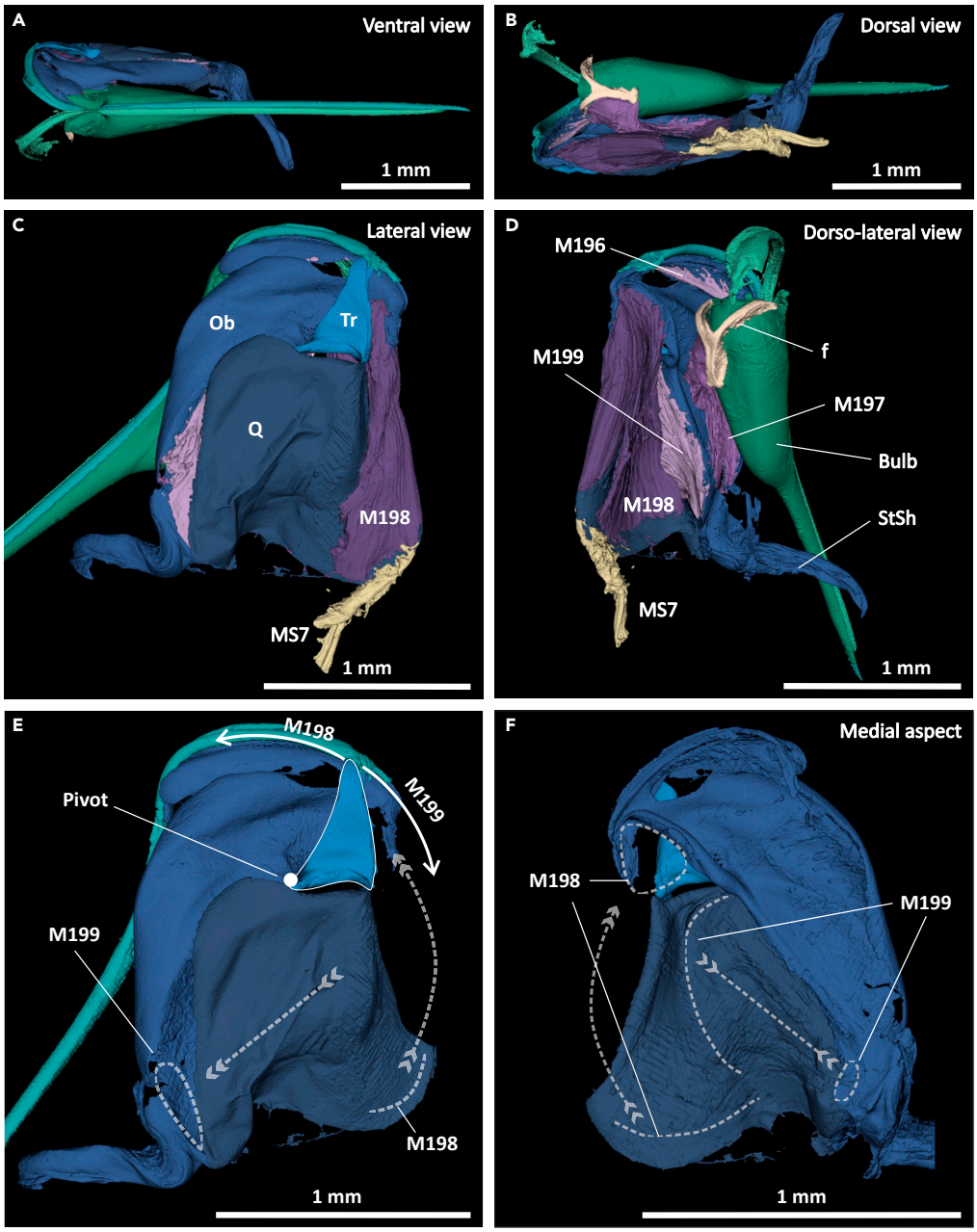

Figure 8. Micro-CT render displaying the muscles and muscle attachment sites of the stinger

(A) Ventral view.

(B) Dorsal view.

(C) Lateral view.

(D) Dorso-lateral view. Muscle M196 connects the oblong plate (Ob) and the anterior margin of the bulb; M197 connects the oblong plate and the furcula (f); M198 and M199 connect the oblong and quadrate plate (Q). The stinger sheath is continuous with the oblong plate (StSh), the quadrate plate is connected to segment 7 via the muscle MS7.

(E) Lateral view of the accessory plates showing the muscle attachment sites (hatched lines), the overall direction of movement resulting from muscle contraction (hatched arrows), and the pivoting direction of the triangular plate accompanying muscle contractions (solid arrows).

(F) Medial aspect of the accessory plates.

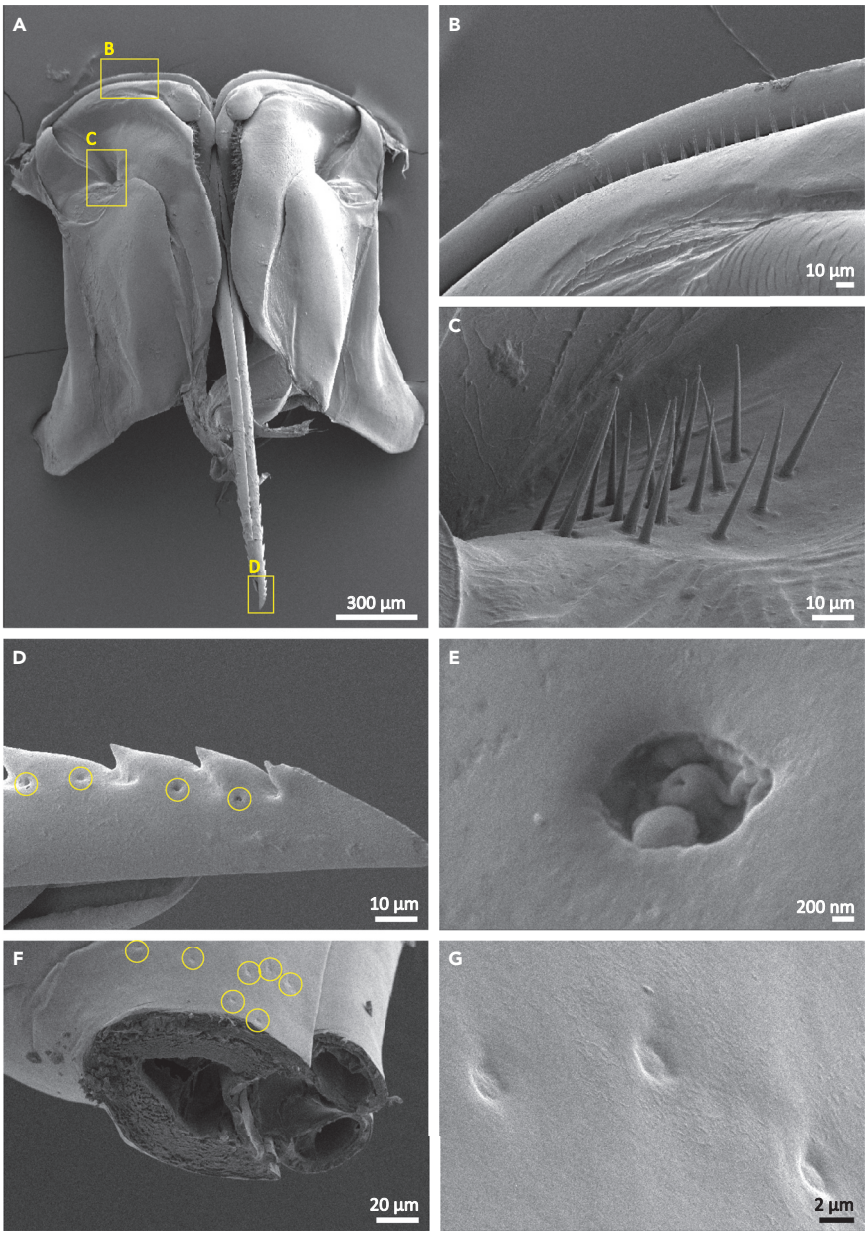

Figure 9. Sensory sensilla on different parts of the stinger

(A) Overview of the stinger displaying sensilla locations.

(B) Hair plate sensilla on the rami.

(C) Hair plate sensilla on the oblong plate.

(D and E) Campaniform sensilla on the tip of the lancet, (F-G) campaniform sensilla on the base of the bulb (note that the insertable length of the stinger has been removed in this preparation).

Hair plate sensilla, or sensilla trichodea, can be observed on the second ramus of the oblong plate (Figures 9A and 9B). These fields contain 24 ± 3.8 sensilla (n = 6), with individual sensory hairs measuring 14 ± 3.1µm (n = 26) in length and 2.3 ± 0.15µm (n = 13) in width. These sensilla are hypothesized to detect movement of the first ramus during extension and retraction of the lancet, these have also been reported by Ogawa et al.[11] and Shing and Erickson.[50] A second field of hair plate sensilla can be found in a concavity of the oblong plate (Figure 9C) close to the triangular plate, this field contains 21 ± 3.5µm (n = 2) sensilla (length = 30 ± 3.7µm, width = 2.6 ± 0.37µm, n = 30). Due to their location, these sensilla are thought to detect the relative position of the triangular plate.[11]

A third field of hair plate sensilla is reported by Ogawa et al.[11] located within the lancet valve. The authors hypothesized that these provide sensory feedback relating to fluid pressure of the venom during stinging. These sensilla were not observed in a previous report by Shing and Erikson,[50] and we were unable to confirm their presence in our imaging.

Campaniform sensilla are present at the base of barbs (2–7) of the lancet and on the lateral margins of the stylet from the distal tip to the base of the bulb (see Figures 9D–9G). Neurons from the campaniform sensilla extend along the lancet and enter the TAG.[9,11,25] Electrophysiological experiments have revealed that stimulations of these sensilla elicit aggressive lancet movements.[11] These sensilla respond to the flexure of the lancets and provide sensory feedback to coordinate penetration of the stinger into the target. There may also be an additional field of campaniform sensilla on the second ramus of the stinger. This was not described by Ogawa et al.[11] but it is sometimes present in other hymenopterans,[38,51] our SEMs displayed some indistinct pitting in the appropriate region but semithin or ultrathin sections of the region would be needed to confirm their presence.

Terminal abdominal ganglion (TAG)

The location and appearance of the TAG has not been clearly described in the literature for the honeybee. However, the gross architecture of the nervous system of the bee stinger, such as the presence of the TAG and its main branches, has been previously described by Ogawa et al.[11,25] To maintain consistency with their work, we will retain their nomenclature in our descriptions. The nerve traces presented here are based on the 3D reconstruction of two micro-CT specimens, a primary specimen (pictured in figures) and a secondary specimen used to confirm some of the more unclear structures. Historically, the TAG and its projections have often been described through diagrammatic illustrations, micro-CT imagery permits measurement of structures and more naturalistic depictions of the *in-situ* appearance of structures in 3D space. This may help future workers wishing to locate specific structures.

3D reconstruction showed that the TAG was located on the proximal end of the stinger apparatus dorsal to the venom sac and is enshrouded by what appeared to be a fine layer of connective tissue, which we have called the TAG shroud (Figure 10A). The body of the ganglion resembled an equilateral triangle with beveled tips and measured approximately 170 × 170 × 60μm. Consistent with previous descriptions, one of the points of the TAG pointed posteriorly and terminated in the connecting branches that, in the intact specimen, would connect to abdominal ganglion 6 (Figures 10B and 10C). The two remaining points of the TAG project nerve roots A8 and A9 laterally toward the accessory plates.

A teardrop-shaped cluster of nervous tissue, almost like an additional small ganglion, was observed anteroventral to the TAG (Figures 10C and 10D). This cluster was visible in both specimens examined and measured approximately 90 × 70 × 16μm, considerably thicker than the surrounding branches (A8 and A9 combined measured 7 × 13μm in cross-section) and TAG shroud (maximum thickness = 10μm). Similar to the TAG this structure had three connections one posterior connection to the TAG and two lateral connections that could not be clearly resolved. This structure was not included in Ogawa et al.[25] or.[11] Smith[15] described the *A. mellifera* abdominal ganglia III through V as separate, VI and VII fused and the terminal ganglion as a fusion of VIII-XI; it is possible that the TAG fusion in *A. mellifera* could be incomplete and that the observed cluster may correspond to ganglion XI. Additional studies are needed to clarify the identity of this cluster.

Nerve roots A8 and A9 projected laterally from the TAG and branched to provide connections to all described muscle groups, as well as potentially infiltrating cuticular structures to provide neural connections to the sensory sensilla. A8 and A9 were closely bound together upon exiting the TAG in our main preparation but clearly distinguishable on our secondary specimen.

Nerve root A9 projected anteriorly from the TAG to innervate all muscle groups (Figure 10D). This is consistent with the descriptions of Ogawa et al.[25] The first branch of A9 extends posterolaterally and divides to send a branchlet toward M198 on one side, and then another branchlet toward M199 via M197 on the other. The second major branch projected anteroventrally and fanned out toward the rami and M196. We were able to trace a branchlet from this arborization extending to enter the oblong plate close to the hair plate sensilla. Additionally, the most ventral branchlets possibly reach as far as the anterior end of the bulb. Whether these branchlets penetrate the cuticle to connect with the campaniform sensilla of the stylet or innervates the ventral aspect of M196 or both was unclear in our preparation. However, there is reason

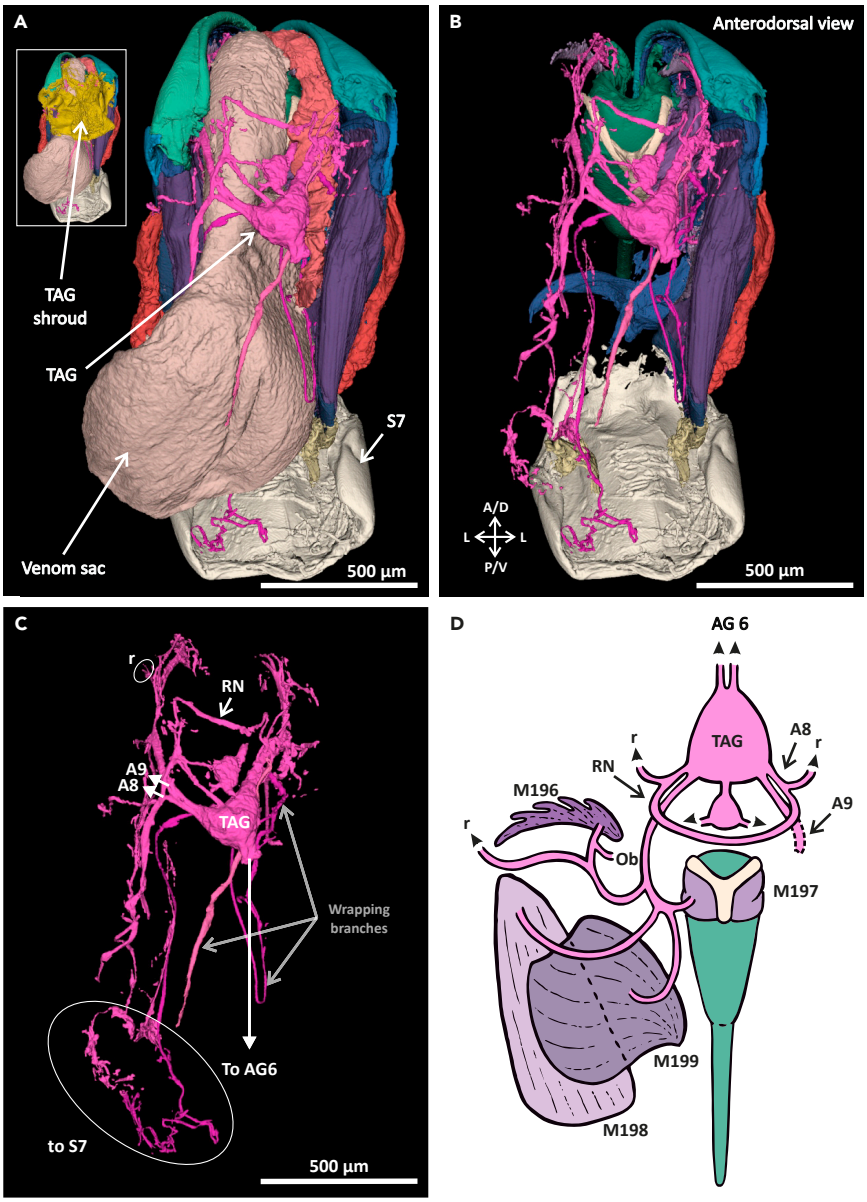

Figure 10. Nervous system of the honeybee stinger

(A) Anterodorsal view of the stinger with all components visible, nervous tissue in pink; inset displays location of the TAG shroud (yellow) that covers the TAG.

(B) Same view of the stinger with glandular tissue, accessory plates, and muscles on one side removed for visibility.

(C) Same view with all components except for neural tissue removed; some nerve branches that are believed to be severed and wrapped around other structures are highlighted.

(D) Diagrammatic illustration of the TAG and its connections (not to scale); note that the TAG is represented as if it had been dissected, flipped, and placed above the bulb in this illustration so that all components could be displayed clearly. A8, A9: root nerve 8 and 9; AG6: Abdominal Ganglion 6; M196: sting retractor muscle; M197: furcula muscle; M198: protractor muscle; M199: retractor muscle; Ob: oblong plate; r: rami; RN: ring nerve; S7: segment 7; TAG: Terminal Abdominal Ganglion.

to believe that this branchlet does enter the bulb since previous literature showed that afferents from the sensory sensilla on the stylet, oblong plate, and stinger sheath enter the TAG via A9.[11]

A posterior branch, likely A8, split to extend to the dorsal tip of the rami and to form a commissure (see "RN" in Figures 10C and 10D). This latter linking branch appears to connect the two A8 branches on either

side of the TAG, this has not previously described in the honeybee but is similar to the ring nerve described in crickets.[52] In crickets the ring nerve serves as a commissure between the two cercal motor neurons.[53] Ogawa et al.[11] trace the afferents from the lancet sensory sensilla to A8, suggesting that the branchlet extending to the rami may carry these afferents.

Other long branches were observed in the micro-CT reconstructions but could not be clearly traced. These most likely extend to S7 and its muscles (see Figure 10C) but for the most part appear to have been damaged in our preparations causing them to wrap around other branches and making it difficult to clearly as certain their origin and termination.

Although no specific staining was used to contrast nervous tissue some of the gross anatomy of the nervous system could be separated in our micro-CT imagery (see Figure 10). We were able to observe the TAG itself and many of its branches, but could not fully resolve terminals or any of the branches that must enter the piercing parts to provide connectivity with the campaniform sensilla found there. The gross anatomy of the nervous system described here was confirmed by partial segmentation of a second specimen. Branches that were not consistent across both specimens (possibly branches damaged during preparation) were left out of the illustration. We report hypothesized connections based on micro-CT data, which are largely consistent with previous literature.[11,15,25,53] Connectivity of the TAG requires further investigation to fully resolve nervous terminals but the expanded diagrammatic representation of stinger neural connections presented here, as well as 3D renders, should assist future endeavors in this area. This is the first three-dimensional reconstruction of the bee TAG and its branches, clearly showing that complex neural connections are preserved in the autotomized stinger.

Glandular components of the stinger

Venom sac and glands

Bee venom is produced in the venom gland (sometimes referred to as the acid gland[54]). This consist of a long filamentous structure located anteriorly to the sting apparatus in the body cavity[22] and terminating at the non-muscularized venom sac[40] (Figure 11A).

Venom is stored in the venom sac until ready to use. Bee venom is chemically complex and its components fluctuate between worker and queen, seasonally, and through the lifespan of the individual.[21,54,55] Approximately 12% of venom is comprised solid material and workers carry approximately 1–2 mg of liquid venom.[21] In micro-CT, we observed the dry venom residue measured 0.125mm^3 (Table S1). Some Hymenoptera, such as certain braconid wasps, possess a muscularized venom sac, which may help to rapidly expel venom.[56] In the honeybee worker, however, only a fine layer of muscle tissue (7.6 $\pm$ 1.8μm, n = 20 in one worker) exists around the venom sac[57] suggesting that venom is mainly delivered through the active motion of the valves on the lancets.[9,58]

Both the gland and the apex of the venom reservoir are lined with secretory cells that excrete venom into the venom sac.[54] Venom production is not a constant process throughout the life of a bee. Workers emerge as adults with an empty venom sac or reservoir, which is gradually filled over the first two weeks of adult life after which they can graduate to serving as hive guards.[54,55,57,59] As workers age the venom glands become atrophied and stop producing venom. This is in contrast with bee queens, which emerge into adulthood with a full venom reservoir. Although workers utilize stinging as a defense strategy to defend the hive from vertebrate and invertebrate aggressors,[7] queens actively attack other queens within the hive to eliminate competition.[60]

Koschevnikov's gland

Prominently visible on the lateral surface of the quadrate plate as a mass of granular material is the Koschevnikov's gland (Figures 8 and 11). This gland is responsible for producing alarm pheromone, which workers emit to recruit additional workers to sting aggressors and respond to potential threats.[61] The basal part of the stinger sheath also produces alarm pheromone.[62] The alarm pheromone is secreted and flows into the stinger chamber where it flows onto and impregnates the setaceous membrane that surrounds the bulb (see Figures 12A–12C); this hair covered membrane provides a large surface area to disperse the volatile pheromone.[7,61,63] The setaceous membrane is also highly flexible and inserts into the medial aspect of the oblong plate on the ventral margin.

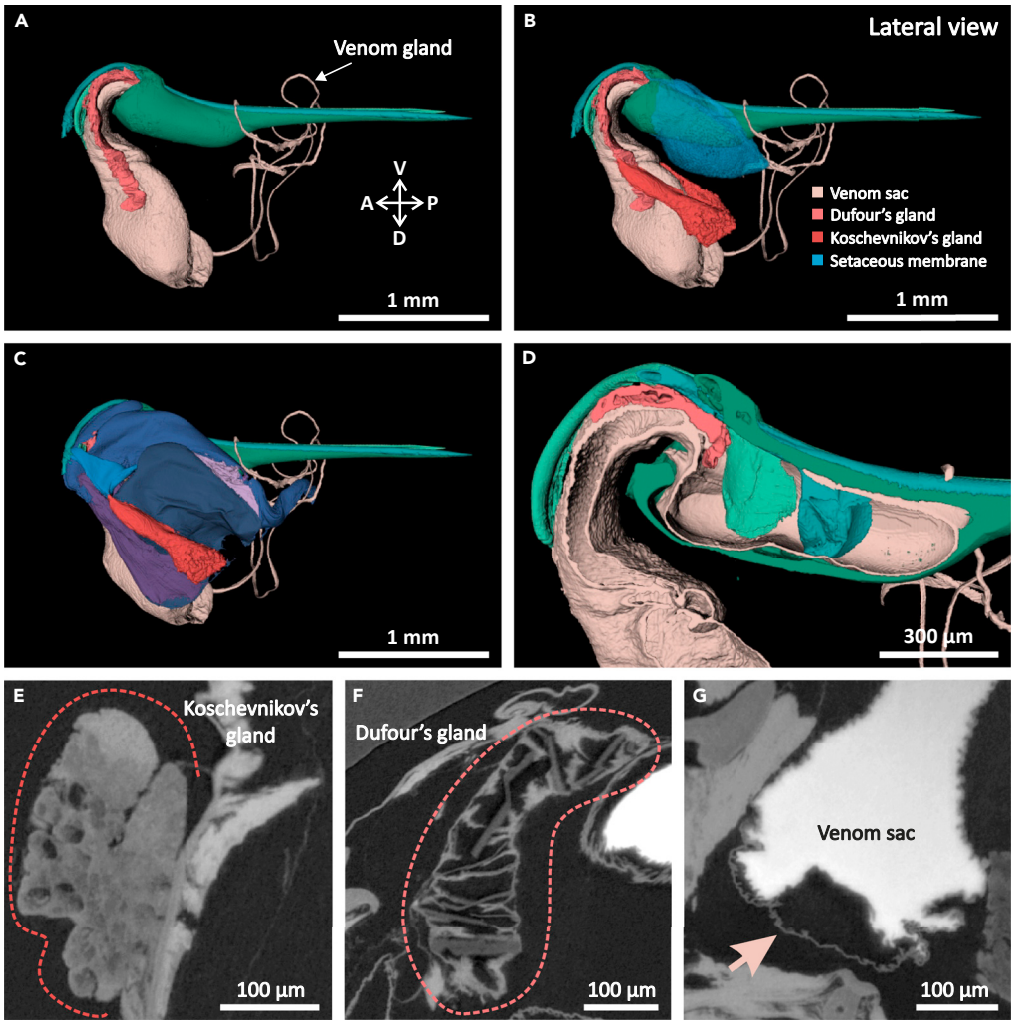

Figure 11. Glandular tissue of the stinger

(A) Micro-CT of the stinger with left plates and muscles removed to reveal the venom sac and Dufour's gland.
(B) All glandular components of the stinger (other than the stinger sheath), note the unpaired Dufour's gland.
(C) Lateral view with plates and musculature attached showing Koschevnikov's gland attached to the quadrate plate.
(D–G) Optical lateral section showing venom sac and Dufour's gland draining into the bulb. Tomograms of: (E) Koschevnikov's gland; (F) Dufour's gland; (G) venom sac, note that the bright signal from the interior of the sac corresponds to dehydrated venom, which strongly absorbs iodide dye.

Stinger sheath

Each of the oblong plates bears a stinger sheath of very fine flexible cuticle (Figure 12). When at rest the sheaths envelop the insertable length of the stinger. The stinger sheath does not have any direct musculature so as the stinger is extended during stinging the sheath passively disengages from the sting shaft.[64] The stinger sheath is thought to have a number of possible roles in different hymenopterans, which may vary with ovipositor use in each taxon. These roles include cleaning the stinger shaft, stabilizing the piercing parts during the initial phases of piercing/ovipositor insertion, helping to guide insertion and playing a sensory role in identifying oviposition/stinging sites.[35,64,65]

Observations here indicate that due to the stinger sheath's thin flexible nature it often appears shriveled and tends to fold over one another due to shrinkage in dehydrated specimens (Figure 12). The stinger sheaths are covered in fine hairs, the lateral aspects of the sheaths bear sensilla that are thought to provide sensory information,[50,65] while the medial aspect of the sheath bears finer setae that do not appear to be sensory.

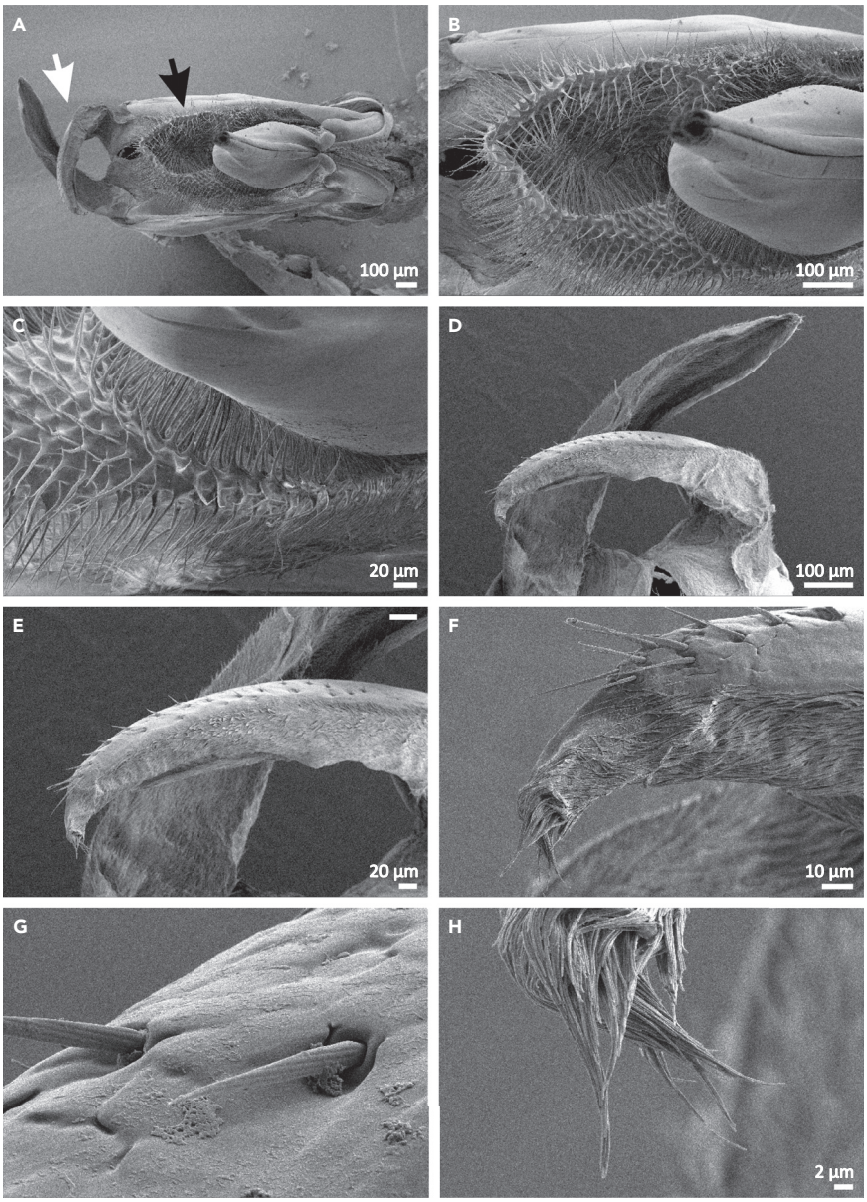

Figure 12. The setaceous membrane and stinger sheath of the stinger

(A) The setaceous membrane (black arrow) is nestled between the accessory plates while the stinger sheath (white arrow) is connected to the oblong plate.

(B and C) The setaceous membrane is a flexible, compliant membrane lined with long setae that wraps around the bulb of the stinger.

(D) The stinger sheaths surround the insertable length of the stinger at rest, in SEM these thin structures shrink and retract from the stinger, folding over each other.

(E) The stinger sheath is covered in fine hairs.

(F–H) The lateral aspects of the stinger sheath bear mechanosensory sensilla (G) while the medial aspects bear finer setae (H).

Dufour's gland

The Dufour's gland also accompanies the stinger upon autotomy (see Figure 11). Although not very obvious it is closely associated with the venom canal connecting the venom sac to the bulb. Some confusion about its function and secretion point exists in older literature, where it is referred to as the basic or alkaline gland. Despite recent studies attempting to ascertain the purpose of the Dufour gland, its function

is still unclear.[66–68] Although in other insects the analogous gland is associated with secreting substances that protect the egg, in Hymenoptera its function seems to have been modified for the production of various semiochemicals.[68] In the bee Martin et al.[69] present histological evidence that points to the gland exiting between the lancets close to the setaceous membrane, indicating that the gland secretions do not drain into the bulb.

Conclusions

Despite its small size the honeybee stinger is a complex structure. This study brings together original 2D and 3D high resolution imaging, and synthesizes recent literature to provide a comprehensive overview of the stinger functional anatomy. Although many unique adaptations of the ovipositor exist in the Hymenoptera the bee stinger is an interesting example of specialization for vertebrate predator deterrence.[2] It exhibits certain unique adaptations, such as pronounced rearward facing barbs that cannot be sheathed (which aid in tissue penetration and make the stinger removal difficult), as well as the ability to undergo autotomy. Stingers observed in this study, which were all artificially autotomized, did not seem to undergo any major damage and even fragile tissues such as neural connections seemed to survive autotomy with all major branches intact.

The bee stinger is derived from a modified ovipositor and has the unique capability of acting autonomously from the bee body. The autotomized stinger carries with it all necessary components to carry out the task of piercing into tissue, pumping venom, and recruiting additional workers to attack an invader. This feature, in combination with the ubiquity of honeybees, makes the bee stinger an interesting study system as it permits unobstructed observation of the stinging mechanics. Previous works have shed much light on the complex system of muscular contractions and accessory plate displacement behind lancet protraction and retraction.[25,35] However, there is still scope to expand our understanding of piercing kinematics by experimentally testing features, such as barb geometries and different lancet activation regimes. Furthermore, the pumping behavior of the valves and fluid kinematics within the bulb are not well understood. The honeybee stinger presents itself as an interesting model to further these studies as well as inform the design of biologically inspired artificial devices, such as medical micro-needles, adhesive patches, and surgical tools.[70–75]

Limitations of the study

This study primarily focused on the static anatomy of the stinger. Although high-speed videography was referenced to interpret the static anatomy here the stinging kinematics and fluid flow characteristics needs further investigation.

Imaging and measurements were carried out on workers of a single hive, as such some size variability in traits might be expected when studying workers of other hive. However, comparisons with previous literature on *A. mellifera* and other related species indicate that the key morphological features described herein should be representative of the species.

Finally, no histological studies were carried out as part of this study, micro-CT alone provides limited insights into the anatomy of the glandular components of the stinger.

STAR★METHODS

Detailed methods are provided in the online version of this paper and include the following:

- KEY RESOURCES TABLE
- RESOURCE AVAILABILITY
  - Lead contact
  - Materials availability
  - Data and code availability
- EXPERIMENTAL MODEL AND STUDY PARTICIPANT DETAILS
- METHOD DETAILS
  - Light microscopy
  - High-speed videography
  - SEM
  - Micro-CT

SUPPLEMENTAL INFORMATION

Supplemental information can be found online at https://doi.org/10.1016/j.isci.2023.107103.

ACKNOWLEDGMENTS

We would like to thank the three anonymous reviewers for detailed comments and feedback which greatly improved this manuscript. Paul Cooper was instrumental in obtaining micro-CT data for this study and we would like to acknowledge his generous help and guidance with sample preparation. We would also like to thank Ajay Narendra (Macquarie University), Jochen Zeil (ANU), and Ryszard Maleszka (ANU) for access to facilities and hosting Fiorella Ramirez Esquivel as a visitor. We would also like to acknowledge technical support from the Centre for Advanced Microscopy and the micro-CT unit at ANU, especially Levi Beeching for micro-CT imaging and guidance. Additional technical assistance from Quinn Graco was invaluable in producing 3D printed models. This work was supported by grant N62909-20-1-2088 from the Office of Naval Research Global.

AUTHOR CONTRIBUTIONS

Conceptualization, F.R.E. and S.R.; Methodology, F.R.E.; Investigation, F.R.E.; Writing – Original Draft, F.R.E.; Writing – Review & Editing, F.R.E. and S.R.; Visualization, F.R.E.; Supervision, S.R.; Funding Acquisition, S.R.

DECLARATION OF INTERESTS

The authors declare no competing interests.

INCLUSION AND DIVERSITY

We support inclusive, diverse, and equitable conduct of research.

Received: December 6, 2022
Revised: March 9, 2023
Accepted: June 8, 2023
Published: June 24, 2023

REFERENCES

1. Wilson, E.O. (1971). The Insect Societies (Harvard University Press).

2. Schmidt, J.O. (2014). Evolutionary responses of solitary and social Hymenoptera to predation by primates and overwhelmingly powerful vertebrate predators. J. Hum. Evol. *71*, 12–19. https://doi.org/10.1016/j.jhevol.2013.07.018.

3. O'Brien, J.M., and Marsh, R.E. (1990). Vertebrate pests of beekeeping. In Proceedings of the 14th Vertebrate Pest Conference, L. Davis and R.E. Marsh, eds. (University of California), pp. 228–232.

4. Shorter, J.R., and Rueppell, O. (2012). A review on self-destructive defense behaviors in social insects. Insectes Soc. *59*, 1–10. https://doi.org/10.1007/s00040-011-0210-x.

5. Schmidt, J.O. (2020). Decision making in honeybees: a time to live, a time to die? Insectes Soc. *67*, 337–344. https://doi.org/10.1007/s00040-020-00759-4.

6. Breed, M.D., Guzmán-Novoa, E., and Hunt, G.J. (2004). Defensive behavior of honey bees: Organization, genetics, and comparisons with other bees. Annu. Rev. Entomol. *49*, 271–298. https://doi.org/10.1146/annurev.ento.49.061802.123155.

7. Nouvian, M., Reinhard, J., and Giurfa, M. (2016). The defensive response of the honeybee *Apis mellifera*. J. Exp. Biol. *219*, 3505–3517. https://doi.org/10.1242/jeb.143016.

8. Vollrath, F., and Douglas-Hamilton, I. (2002). African bees to control African elephants. Naturwissenschaften *89*, 508–511. https://doi.org/10.1007/s00114-002-0375-2.

9. Snodgrass, R.E. (1910). The Anatomy of the Honey Bee. Nature *85*, 169. https://doi.org/10.1038/085169b0.

10. Alba-Tercedor, J., and Bartomeus, I. (2016). Micro-CT as a tool straddling scientist research, art and education. Study of *Osmia* sp., a mason bee (Insecta, Hymenoptera: Megachilidae). In Bruker Micro-CT Users Meeting 2016, B. Micro-CT, ed., pp. 74–91.

11. Ogawa, H., Kawakami, Z., and Yamaguchi, T. (2011). Proprioceptors involved in stinging response of the honeybee, *Apis mellifera*. J. Insect Physiol. *57*, 1358–1367. https://doi.org/10.1016/j.jinsphys.2011.07.003.

12. Zhao, Z.L., Zhao, H.P., Ma, G.J., Wu, C.W., Yang, K., and Feng, X.Q. (2015). Structures, properties, and functions of the stings of honey bees and paper wasps: A comparative study. Biol. Open *4*, 921–928. https://doi.org/10.1242/bio.012195.

13. Das, R., Yadav, R.N., Sihota, P., Uniyal, P., Kumar, N., and Bhushan, B. (2018). Biomechanical evaluation of wasp and honeybee stingers. Sci. Rep. *8*, 1–13. https://doi.org/10.1038/s41598-018-33386-y.

14. Ling, J., Song, Z., Wang, J., Chen, K., Li, J., Xu, S., Ren, L., Chen, Z., Jin, D., and Jiang, L. (2017). Effect of honeybee stinger and its microstructured barbs on insertion and pull force. J. Mech. Behav. Biomed. Mater. *68*, 173–179. https://doi.org/10.1016/j.jmbbm.2017.01.040.

15. Smith, E.L. (1970). Evolutionary morphology of the external insect genitalia. 2. Ann. Entomol. Soc. Am. *63*, 1–27. https://doi.org/10.1093/aesa/63.1.1.

16. Piek, T. (2013). Morphology of the venom apparatus. In Venoms of the Hymenoptera: biochemical, pharmacological and behavioural aspects, T. Piek, ed. (Elsevier).

17. Blaimer, B.B., Santos, B.F., Cruaud, A., Gates, M.W., Kula, R.R., Mikó, I., Rasplus, J., Smith, D.R., Talamas, E.J., Brady, S.G., et al. (2023). Key innovations and the diversification of

Hymenoptera. Nat. Commun. *14*, 1212. https://doi.org/10.1038/s41467-023-36868-4.

18. Hermann, H.R. (1971). Sting autotomy, a defensive mechanism in certain social Hymenoptera. Insectes Soc. *18*, 111–120. https://doi.org/10.1007/BF02223116.

19. Sakagami, S.F., and Akahira, Y. (1960). Studies on the Japanese Honeybee, Apis cerana cerana Fabricius. VIII. Two Opposing Adaptations in the Post-Stinging Behavior of Honeybees. Evolution *14*, 29. https://doi.org/10.2307/2405920.

20. Cunard, S.J., and Breed, M.D. (1998). Post-stinging behavior of worker honey bees (Hymenoptera: Apidae). Ann. Entomol. Soc. Am. *91*, 754–757. https://doi.org/10.1093/aesa/91.5.754.

21. Banks, B.E., and Shipolini, R.A. (1986). Chemistry and pharmacology of honey-bee venom. Venoms Hymenopt, 329–416. https://doi.org/10.1016/b978-0-12-554770-3.50011-5.

22. Snodgrass, R.E. (1956). Anatomy of the Honey Bee (Cornell University Press).

23. Cerkvenik, U., Van De Straat, B., Gussekloo, S.W.S., and Van Leeuwen, J.L. (2017). Mechanisms of ovipositor insertion and steering of a parasitic wasp. Proc. Natl. Acad. Sci. USA *114*, E7822–E7831. https://doi.org/10.1073/pnas.1706162114.

24. Vincent, J.F.V., and King, M.J. (1995). The mechanism of drilling by wood wasp ovipositors. Biomimetics *3*, 187–201.

25. Ogawa, H., Kawakami, Z., and Yamaguchi, T. (1995). Motor pattern of the stinging response in the honeybee Apis mellifera. J. Exp. Biol. *198*, 39–47. https://doi.org/10.1242/jeb.198.1.39.

26. Chopra, K., Calva, D., Sosin, M., Tadisina, K.K., Banda, A., De La Cruz, C., Chaudhry, M.R., Legesse, T., Drachenberg, C.B., Manson, P.N., and Christy, M.R. (2015). A comprehensive examination of topographic thickness of skin in the human face. Aesthet. Surg. J. *35*, 1007–1013. https://doi.org/10.1093/asj/sjv079.

27. Oltulu, P., Ince, B., Kökbudak, N., Findik, S., and Kiliç, F. (2018). Measurement of epidermis, dermis, and total skin thicknesses from six different body regions with a new ethical histometric technique. Turk. J. Plast. Surg. *26*, 56–61. https://doi.org/10.4103/tjps.tjps_2_17.

28. Gal, R., Kaiser, M., Haspel, G., and Libersat, F. (2014). Sensory arsenal on the stinger of the parasitoid jewel wasp and its possible role in identifying cockroach brains. PLoS One *9*, e89683. https://doi.org/10.1371/journal.pone.0089683.

29. Quicke, D.L.J., Fitton, M.G., Tunstead, J.R., Ingram, S.N., and Gaitens, P.V. (1994). Ovipositor structure and relationships within the Hymenoptera, with special reference to the Ichneumonoidea. J. Nat. Hist. *28*, 635–682. https://doi.org/10.1080/00222939400770301.

30. Baumann, K., Vicenzi, E.P., Lam, T., Douglas, J., Arbuckle, K., Cribb, B., Brady, S.G., and Fry, B.G. (2018). Harden up: metal acquisition in the weaponized ovipositors of aculeate hymenoptera. Zoomorphology *137*, 389–406. https://doi.org/10.1007/s00435-018-0403-1.

31. Ramya, J., and Rajagopal, D. (2008). Morphology of the sting and its associated glands in four different honey bee species. J. Apic. Res. *47*, 46–52. https://doi.org/10.1080/00218839.2008.11101422.

32. Surendra, N.S., Jayaram, G.N., Reddy, M.R.S., and Ravikumar, H. (2013). Comparative morphometric studies of the sting apparatus of the worker bees of four different *Apis* species (*Apis dorsata, Apis mellifera, Apis cerana* and *Apis florea*). J. Apic. Res. *52*, 74–80. https://doi.org/10.3896/IBRA.1.52.2.16.

33. Mulfinger, L., Yunginger, J., Styer, W., Guralnick, M., and Lintner, T. (1992). Sting morphology and frequency of sting autotomy among medically important vespids (Hymenoptera: Vespidae) and the honey bee (Hymenoptera: Apidae). J. Med. Entomol. *29*, 325–328. https://doi.org/10.1093/jmedent/29.2.325.

34. Bissessarsingh, M., and Starr, C.K. (2021). Comparative morphology of the stinger in social wasps (Hymenoptera: Vespidae). Insects *12*, 1–10. https://doi.org/10.3390/insects12080729.

35. van Meer, N.M.M.E., Cerkvenik, U., Schlepütz, C.M., van Leeuwen, J.L., and Gussekloo, S.W.S. (2020). The ovipositor actuation mechanism of a parasitic wasp and its functional implications. J. Anat. *237*, 689–703. https://doi.org/10.1111/joa.13216.

36. Csader, M., Mayer, K., Betz, O., Fischer, S., and Eggs, B. (2021). Ovipositor of the braconid wasp *Habrobracon hebetor*: Structural and functional aspects. J. Hymenopt. Res. *83*, 73–99. https://doi.org/10.3897/jhr.83.64018.

37. Matushkina, N.A., and Stetsun, H.A. (2016). Morphology of the sting apparatus of the digger wasp *Oxybelus uniglumis* (Linnaeus, 1758) (Hymenoptera, Crabronidae), with emphasis on intraspecific variability and behavioural plasticity. Insect Systemat. Evol. *47*, 347–362. https://doi.org/10.1163/1876312X-47032146.

38. Matushkina, N. (2011). Sting microsculpture in the digger wasp *Bembix rostrata* (Hymenoptera, Crabronidae). J. Hymenopt. Res. *21*, 41–52. https://doi.org/10.3897/JHR.21.873.

39. Weyda, F., and Kodrík, D. (2020). New functionally ultrastructural details of the honey bee stinger tip: serrated edge and pitted surface. J. Apic. Res. *60*, 875–878. https://doi.org/10.1080/00218839.2020.1837545.

40. Maschwitz, U.W.J., and Kloft, W. (1971). Morphology and Function of the Venom Apparatus of Insects—Bees, Wasps, Ants, and Caterpillars. In Venomous Animals and their Venoms, pp. 1–60. https://doi.org/10.1016/b978-0-12-138903-1.50008-9.

41. Manzoli-Palma, M., and Gobbi, N. (1997). Sting autotomy, sting morpholology and sociality in Neotropical Vespids (Hymenoptera: Vespidae). J. Hymenopt. Res. *6*, 152–162.

42. Sledge, M.F., Dani, F.R., Fortunato, A., Maschwitz, U., Clarke, S.R., Francescato, E., Hashim, R., Morgan, E.D., Jones, G.R., and Turillazzi, S. (1999). Venom induces alarm behaviour in the social wasp *Polybioides raphigastra* (Hymenoptera: Vespidae): An investigation of alarm behaviour, venom volatiles and sting autotomy. Physiol. Entomol. *24*, 234–239. https://doi.org/10.1046/j.1365-3032.1999.00137.x.

43. Greene, A., Breisch, N.L., Golden, D.B.K., Kelly, D., and Douglass, L.W. (2012). Sting embedment and avulsion in yellowjackets (Hymenoptera: Vespidae): A functional equivalent to autotomy. Am. Entomol. *58*, 50–57. https://doi.org/10.1093/ae/58.1.0050.

44. Packer, L. (2003). Comparative morphology of the skeletal parts of the sting apparatus of bees (Hymenoptera: Apoidea). Zool. J. Linn. Soc. *138*, 1–38. https://doi.org/10.1046/j.1096-3642.2003.00055.x.

45. Austin, A.D., and Browning, T.O. (1981). A mechanism for movement of eggs along insect ovipositors. Int. J. Insect Morphol. Embryol. *10*, 93–108. https://doi.org/10.1016/S0020-7322(81)80015-3.

46. Quicke, D.L.J., Fitton, M.G., and Ingram, S. (1992). Phylogenetic implications of the structure and distribution of ovipositor valvilli in the Hymenoptera (Insecta). J. Nat. Hist. *26*, 587–608. https://doi.org/10.1080/00222939200770361.

47. Hermann, H.R., and Willer, D.E. (1986). Resilin distribution and its function in the venom apparatus of the honey bee, *Apis mellifera* L. (Hymenoptera : Apedae). Int. J. Insect Morphol. Embryol. *15*, 107–114. https://doi.org/10.1016/0020-7322(86)90011-5.

48. Boring, C.A., Sharkey, M.J., and Nychka, J.A. (2009). Structure and functional morphology of the ovipositor of *Homolobus truncator* (hymenoptera: Ichneumonoidea: Braconidae). J. Hymenopt. Res. *18*, 1–24.

49. Eggs, B., Birkhold, A.I., Röhrle, O., and Betz, O. (2018). Structure and function of the musculoskeletal ovipositor system of an ichneumonid wasp. BMC Zool *3*, 1–25. https://doi.org/10.1186/s40850-018-0037-2.

50. Shing, H., and Erickson, E.H. (1982). Some ultrastructure of the honeybee (*Apis mellifera* L.) sting. Apidologie *13*, 203–213.

51. Stetsun, H., and Matushkina, N.A. (2020). Sting morphology of the European hornet, *Vespa crabro* L., (Hymenoptera: Vespidae) re-examined. Entomol. Sci. *23*, 416–429. https://doi.org/10.1111/ens.12438.

52. Insausti, T.C., Lazzari, C.R., and Casas, J. (2008). The terminal abdominal ganglion of the wood cricket *Nemobius sylvestris*. J. Morphol. *269*, 1539–1551. https://doi.org/10.1002/jmor.10672.

53. Killian, K.A., Bollins, J.P., and Govind, C.K. (2000). Anatomy and physiology of neurons composing the commissural ring nerve of the cricket, *Acheta domesticus*. J. Exp. Zool. *286*, 350–366. https://doi.org/10.1002/(SICI)1097-010X(20000301)286:4<350::AID-JEZ3>3.0.CO;2-3.

54. Owen, M.D., and Bridges, A.R. (1976). Aging in the venom glands of queen and worker honey bees (*Apis mellifera* L.): Some morphological and chemical observations. Toxicon *14*, 1–5. https://doi.org/10.1016/0041-0101(76)90113-6.

55. Owen, M.D., and Pfaff, L.A. (1995). Melittin synthesis in the venom system of the honey bee (*Apis mellifera* L.). Toxicon *33*, 1181–1188. https://doi.org/10.1016/0041-0101(95)00054-.

56. Edson, K.M., Barlin, M.R., and Vinson, S.B. (1982). Venom apparatus of braconid wasps: comparative ultrastructure of reservoirs and gland filaments. Toxicon *20*, 553–562. https://doi.org/10.1016/0041-0101(82)90049-6.

57. Bridges, A.R., and Owen, M.D. (1984). The morphology of the honey bee (*Apis mellifera* L.) venom gland and reservoir. J. Morphol. *181*, 69–86. https://doi.org/10.1002/jmor.1051810107.

58. Goodman, L. (2003). Form and Function in the Honey Bee (International Bee Research Association).

59. Bachmayer, H., Kreil, G., and Suchanek, G. (1972). Synthesis of promelittin and melittin in the venom gland of queen and worker bees: Patterns observed during maturation. J. Insect Physiol. *18*, 1515–1521. https://doi.org/10.1016/0022-1910(72)90230-2.

60. Gilley, D.C. (2001). The behavior of honey bees (*Apis mellifera ligustica*) during queen duels. Ethology *107*, 601–622. https://doi.org/10.1046/j.1439-0310.2001.00692.x.

61. Grandperrin, D., and Cassier, P. (1983). Anatomy and ultrastructure of the Koschewnikov's gland of the honey bee, *Apis mellifera* L. (Hymenoptera: Apidae). Int. J. Insect Morphol. Embryol. *12*, 25–42. https://doi.org/10.1016/0020-7322(83)90033-8.

62. Cassier, P., Tel-Zur, D., and Lensky, Y. (1994). The sting sheaths of honey bee workers (*Apis mellifera* L.): Structure and alarm pheromone secretion. J. Insect Physiol. *40*, 23–32. https://doi.org/10.1016/0022-1910(94)90108-2.

63. Lensky, Y., Cassier, P., and Tel-Zur, D. (1995). The setaceous membrane of honey bee (*Apis mellifera* L.) workers' sting apparatus: Structure and alarm pheromone distribution. J. Insect Physiol. *41*, 589–595. https://doi.org/10.1016/0022-1910(95)00007-H.

64. Kumpanenko, A., Gladun, D., and Vilhelmsen, L. (2019). Functional morphology and evolution of the sting sheaths in Aculeata (Hymenoptera). Arthropod Syst. Phylogeny *77*, 325–338. https://doi.org/10.26049/ASP77-2-2019-08.

65. Vilhelmsen, L. (2003). Flexible ovipositor sheaths in parasitoid Hymenoptera (Insecta). Arthropod Struct. Dev. *32*, 277–287. https://doi.org/10.1016/S1467-8039(03)00045-8.

66. Katzav-Gozansky, T., Ibarra, F., Francke, W., Hefetz, A., and Soroker, V. (2001). Dufour's gland secretion of the queen honeybee (*Apis mellifera*): An egg discriminator pheromone or a queen signal? Behav. Ecol. Sociobiol. *51*, 76–86. https://doi.org/10.1007/s002650100406.

67. Martin, S.J., Jones, G.R., Châline, N., Middleton, H., and Ratnieks, F.L.W. (2002). Reassessing the role of the honeybee (*Apis mellifera*) Dufour's gland in egg marking. Naturwissenschaften *89*, 528–532. https://doi.org/10.1007/s00114-002-0367-2.

68. Abdalla, F.C., and da Cruz-Landim, C. (2001). Dufour glands in the hymenopterans (Apidae, Formicidae, Vespidae): a review. Braz. J. Biol. *61*, 95–106. https://doi.org/10.1590/s0034-71082001000100013.

69. Martin, S.J., Dils, V., and Billen, J. (2005). Morphology of the Dufour gland within the honey bee sting gland complex. Apidologie *36*, 543–546. https://doi.org/10.1051/apido:2005041.

70. Sahlabadi, M., Gardell, D., Attia, J.Y., Khodaei, S., and Hutapea, P. (2017). Insertion mechanics of 3D printed honeybee-inspired needle prototypes for percutaneous procedure. In Frontiers in Biomedical Devices (American Society of Mechanical Engineers). V001T08A020.

71. Chen, Z., Lin, Y., Lee, W., Ren, L., Liu, B., Liang, L., Wang, Z., and Jiang, L. (2018). Additive manufacturing of honeybee-inspired microneedle for easy skin insertion and difficult removal. ACS Appl. Mater. Interfaces *10*, 29338–29346. https://doi.org/10.1021/acsami.8b09563.

72. Tran, L.G., Nguyen, T.Q., and Park, W.T. (2019). Bio-inspired barbed microneedle for skin adhesion with interlocking mechanics. Proc. IEEE Int. Conf. Micro Electro Mech. Syst. *2019-Janua*, 547–550. https://doi.org/10.1109/MEMSYS.2019.8870874.

73. Sakes, A., van de Steeg, I.A., de Kater, E.P., Posthoorn, P., Scali, M., and Breedveld, P. (2020). Development of a novel wasp-inspired friction-based tissue transportation device. Front. Bioeng. Biotechnol. *8*, 575007–575011. https://doi.org/10.3389/fbioe.2020.575007.

74. Gao, Y., Ellery, A., Sweeting, M.N., and Vincent, J. (2007). Bioinspired drill for planetary sampling: Literature survey, conceptual design, and feasibility study. J. Spacecraft Rockets *44*, 703–709. https://doi.org/10.2514/1.23025.

75. Ko, S.Y., Frasson, L., and Rodriguez Y Baena, F. (2011). Closed-loop planar motion control of a steerable probe with a programmable bevel inspired by nature. IEEE Trans. Robot. *27*, 970–983. https://doi.org/10.1109/TRO.2011.2159411.

76. Ling, J., Jiang, L., Chen, K., Pan, C., Li, Y., Yuan, W., and Liang, L. (2016). Insertion and pull behavior of worker honeybee stinger. J. Bionic Eng. *13*, 303–311. https://doi.org/10.1016/S1672-6529(16)60303-7.

77. Kingston, A.M., Myers, G.R., Latham, S.J., Recur, B., Li, H., and Sheppard, A.P. (2018). Space-filling x-ray source trajectories for efficient scanning in large-angle cone-beam computed tomography. IEEE Trans. Comput. Imaging *4*, 447–458. https://doi.org/10.1109/tci.2018.2841202.

78. Myers, G.R., Kingston, A.M., Varslot, T.K., and Sheppard, A.P. (2011). Extending reference scan drift correction to high-magnification high-cone-angle tomography. Opt. Lett. *36*, 4809–4811. https://doi.org/10.1364/OL.36.004809.

79. Latham, S.J., Varslot, T., and Sheppard, A. (2008). Automated registration for augmenting micro-CT 3D images. ANZIAM J. *50*, C534–C548. https://doi.org/10.21914/anziamj.v50i0.1389.

80. Schindelin, J., Arganda-Carreras, I., Frise, E., Kaynig, V., Longair, M., Pietzsch, T., Preibisch, S., Rueden, C., Saalfeld, S., Schmid, B., et al. (2012). Fiji: an open-source platform for biological-image analysis. Nat. Methods *9*, 676–682. https://doi.org/10.1038/NMETH.2019.

81. Yushkevich, P.A., Piven, J., Hazlett, H.C., Smith, R.G., Ho, S., Gee, J.C., and Gerig, G. (2006). User-guided 3D active contour segmentation of anatomical structures: Significantly improved efficiency and reliability. Neuroimage *31*, 1116–1128. https://doi.org/10.1016/j.neuroimage.2006.01.015.

82. Cignoni, P., Callieri, M., Corsini, M., Dellepiane, M., Ganovelli, F., and Ranzuglia, G. (2008). MeshLab: An open-source mesh processing tool. 6th Eurographics Ital. Chapter Conf. 2008 - Proc, 129–136. https://doi.org/10.2312/LocalChapterEvents/ItalChap/ItalianChapConf2008/129-136.

STAR★METHODS

KEY RESOURCES TABLE

REAGENT or RESOURCE	SOURCE	IDENTIFIER
Biological samples		
Apis mellifera stingers	Collected from foraging female workers from a managed hive kept at the UNSW Canberra campus	N/A
Chemicals, peptides, and recombinant proteins		
Sodium hydroxide	Australian Scientific	Cat# SL178
Ethanol	Australian Scientific	Cat# EA043
Bouin's solution	ProSciTech	Cat# EMS15990
Lugol's Iodine	ProSciTech	Cat#EMS26369-03
Deposited data		
MicroCT data	MorphoSource	MorphoSource: https://doi.org/10.17602/M2/M478590
Software and algorithms		
Fiji	Schindelin et al.[18]	https://imagej.net/software/fiji/; RRID:SCR_002285
ITK-SNAP	Yushkevich et al.[19]	https://www.itksnap.org/; RRID:SCR_017341
Microsoft Excel	Microsoft, Richmond USA	https://www.microsoft.com
MeshMixer	Autodesk Inc	RRID:SCR_015736
MeshLab	Cignoni et al.[81]	
PrusaSlicer	Prusa Research	
Other		
Silicon rubber (SiliCreate UltraSoft-10)	SiliCreate	N/A
Flexible 3D printing filament TPU 95A (eSun)	Cubic Technology	N/A

RESOURCE AVAILABILITY

Lead contact

Further information and requests for resources should be directed to and will be fulfilled by the lead contact, Fiorella Ramirez Esquivel (f.esquivel@unsw.edu.au).

Materials availability

This study did not generate new unique reagents.

Data and code availability

- micro-CT data have been deposited at MorphoSource and are publicly available as of the date of publication. Accession numbers are listed in the key resources table.
- This paper does not report original code.
- Any additional information required to reanalyse the data reported in this paper is available from the lead contact upon request.

EXPERIMENTAL MODEL AND STUDY PARTICIPANT DETAILS

Foraging honey bee workers were collected from a colony of *A. mellifera* kept at the UNSW Canberra campus.

METHOD DETAILS

Light microscopy

Workers were cold anaesthetised by placing them in a refrigerator (approx. 7°C for 5 minutes). The stingers were then removed by lightly pulling on the insertable length of the stinger using fine forceps, which caused the entire stinger apparatus to come free from the bee abdomen. This was done either under no magnification or under a stereo microscope (Leica, M80). Workers were immediately killed and the stingers were placed in a 10% NaOH solution overnight or until all muscle tissue was dissolved. The stingers were then rinsed in water and stored in 70% ethanol until ready to image. Light microscopy images were captured using a stereomicroscope equipped with a motorised stage for focus stacking (Leica, M205FA). Multifocus images were produced using the inbuilt Leica software (LAS X).

High-speed videography

Stinging behaviour was observed using a stereomicroscope (as above) and illuminated with transmitted illumination from the microscope's light base. Bees were cold anaesthetised (3-4 minutes at 7°C) and stingers removed using forceps. Bees were immediately euthanised after stinger removal. Stingers were observed either with or without a stinging substrate. When presented with a substrate the stingers were partially manually inserted into a small block (approx. 4x2x1mm) of silicon rubber (SiliCreate UltraSoft-10) affixed to a microscope slide. A similar material has been previously used to imitate human skin in bee stinging experiments.[76] Filming was done using a Chronos 2.1-HD (Kron Technologies) high speed camera at 100 frames per second with a spatial resolution of 1280x1024 pixels.

SEM

Specimens were prepared as for light microscopy or directly dissected without digestion. Specimens were then dehydrated in an ethanol series (60, 70, 80, 90, 100%; 10 minutes each) before critical point drying (Balzers CPD 030). Dehydrated samples were mounted on conductive, double-sided, adhesive carbon tabs on aluminium stubs and sputter coated (Au, 2 minutes, 20mA). Specimens were imaged using a Zeiss UltraPlus FESEM under an accelerating voltage of 3kV.

Micro-CT

Sample preparation

Stinger removal was carried out as for light microscopy and stingers placed in cold (4°C) Bouin's solution for at least one day or until ready to proceed. Specimens were then rinsed in 70% ethanol repeatedly until only a slight yellow colouration was observed in the ethanol wash. Samples were stored overnight in ethanol to observe whether further excess Bouin's was still present. Further washes were carried out as needed (preparations which included the venom sac strongly retained Bouin's and many additional washes over several days were required). Specimens were then stained for contrast using Lugol's Iodine (1.25% I_2 & 2.5% KI) for a week. After a week the specimens were rinsed in 70% ethanol and tested for contrast under the micro-CT beamline. Sufficient staining was achieved at this point but stain was retained in the bulb and venom sac. Additional rinses in 70% ethanol were carried out then samples were dehydrated in an ethanol series (70, 80, 90% for ten minutes each then 100% x 3 for 30 minutes each). Finally, five specimens were scanned at the 'National Laboratory for X-ray Micro Computed Tomography (CTLab)' based at the Australian National University (ANU) using a HeliScan Micro-CT system with an optimized space-filling trajectory[77] to yield sharp images[78,79] at a resolution of 1.1μm.

Data analysis

Scan data was imported into Fiji[80] as TIF stacks. Individual stingers were cropped in the X, Y, and Z axes and exported as single NIfTI files. Data was then analysed using ITK-SNAP.[81] Pre-segmentation was done using the 'Classification' tool, which classifies tissue types on the basis of greyscale values (i.e. radio density). Due to the presence of many thin structures and relatively poor density differentiation between tissue types the pre-segmentation was only partially successful in separating muscle, cuticle, and connective tissues. Manual segmentation was required to fully define and separate the different components of the stinger. This was performed using an IntuosPro tablet (Wacom, PTH-651). Segmentations were rendered within ITK-SNAP.

3D printing

In order to visualise geometries of certain stinger components mesh files were exported and 3D printed. Reconstructions were exported from ITK-Snap as .stl mesh files and cleaned up using a combination of MeshMixer (Autodesk Inc., San Rafael, CA, USA) and MeshLab.[82] Files sliced for printing using PrusaSlicer 2.5.0 (Prusa Research a.s., Praha, Czech Republic). Models were printed on a Prusa i3 MK3S^{TM} printer (Prusa Research a.s., Praha, Czech Republic) using a flexible filament (eSun TPU 95A).